

Advancements in AI for Healthcare





Ngoc-Huynh Ho

Postdoctoral Researcher

Department of Artificial Intelligence Convergence

Chonnam National University, South Korea

Who I am



Ngoc-Huynh Ho

1

Current Position – 2021 to present

- Postdoctoral Researcher
- Department of AI Convergence, Chonnam National University, S. Korea

2

Ph.D Degree – 2017 to 2021

- Smart Computing Lab, Department of AI Convergence, Chonnam National University, S. Korea
- Thesis "*A Study on Prediction of Alzheimer's Disease Progression Using Bidirectional-Progressive Recurrent Networks*"

3

MS Degree – 2015 to 2017

- Smart Embedded System Lab, Department of Electrical Engineering, Kookmin University, S. Korea
- Thesis "*Distance Estimation Considering Varying Walking Speed for Smartphone PDR Using Adaptive Step-Length Estimation*"

4

BE Degree – 2010 to 2015

- Department of Telecommunications, Ho Chi Minh City University of Technology, Vietnam
- Thesis "*Impact of Channel Estimation Error on the Performance of Relay Selection in Cognitive Radio Networks*"



Outline

- **Alzheimer’s disease prediction**
  - Non-white Matter AD Detection (2018)
  - Alzheimer's Progression Prediction (2022)
  - Multimodal MCI-to-AD Prediction (2023)

- **Tumor Detection**
  - Knee-bone tumor prediction (2019)
  - Abnormal tissue segmentation (2020)
  - Non-small cell lung cancer prediction (2022)

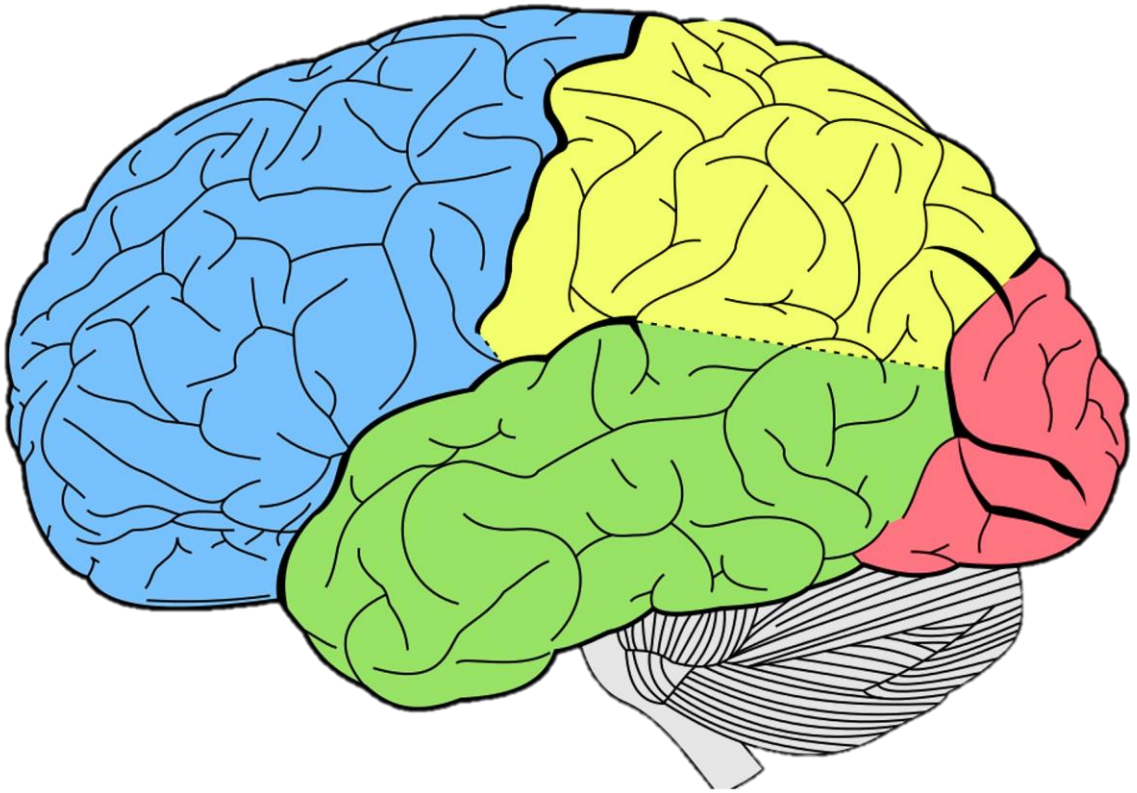


Alzheimer's Disease Prediction

Alzheimer’s disease prediction

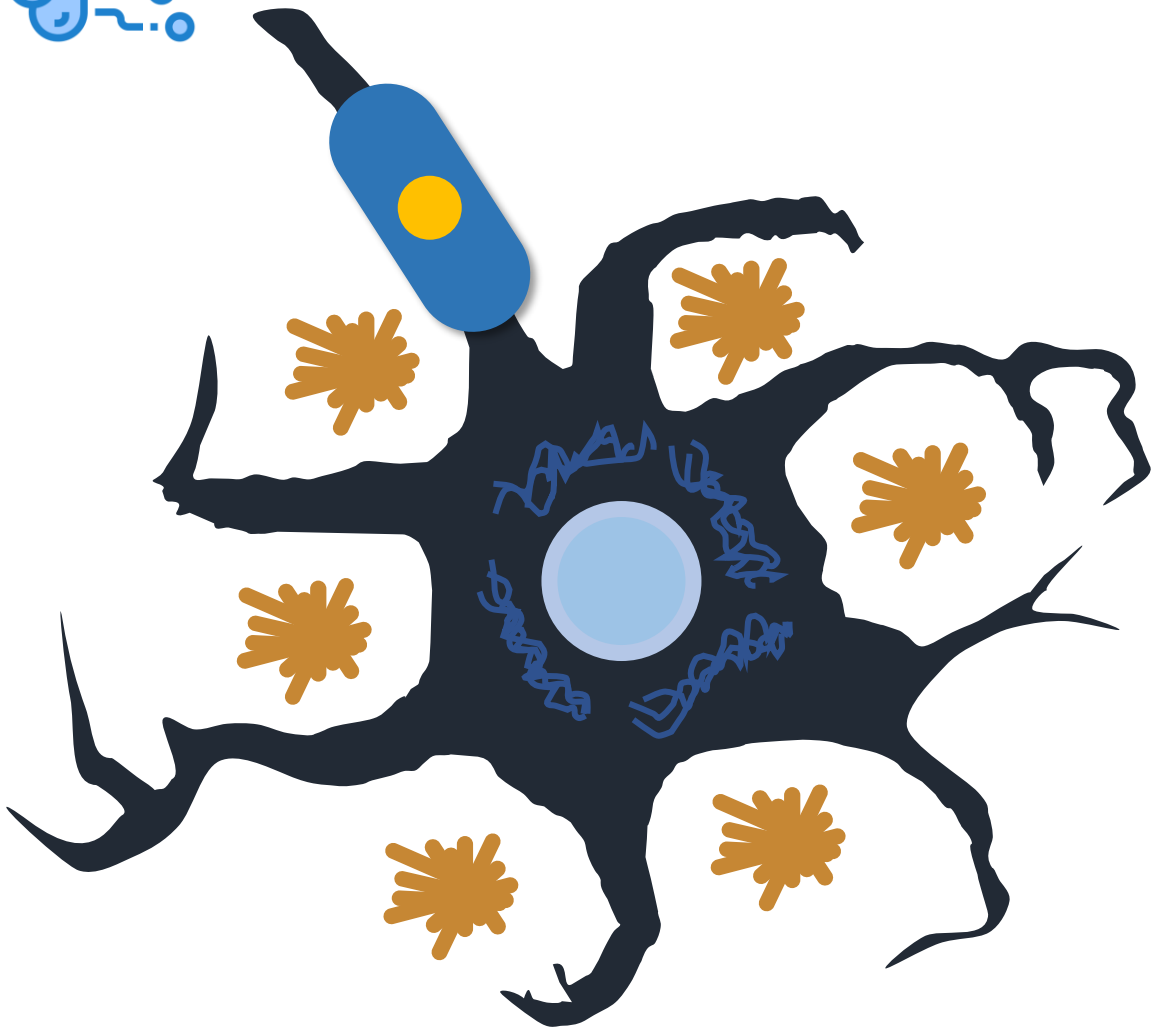
Alzheimer’s disease?

most common cause of dementia



Caused by the formation of the abnormal deposits of protein in the brain

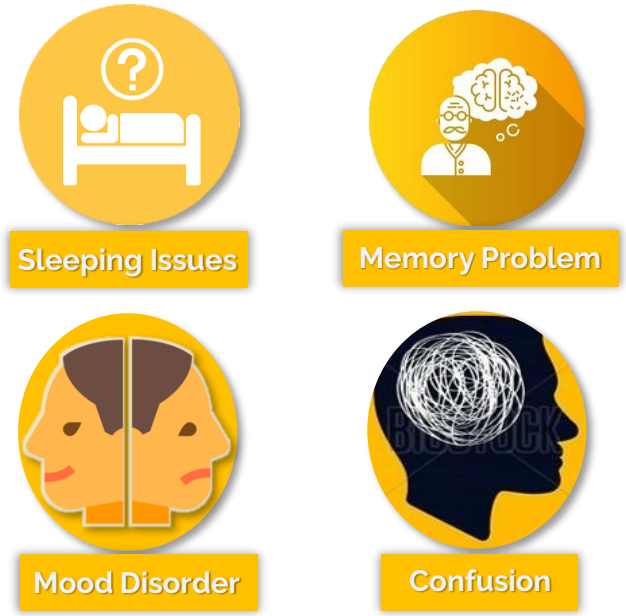
Alzheimer's disease prediction



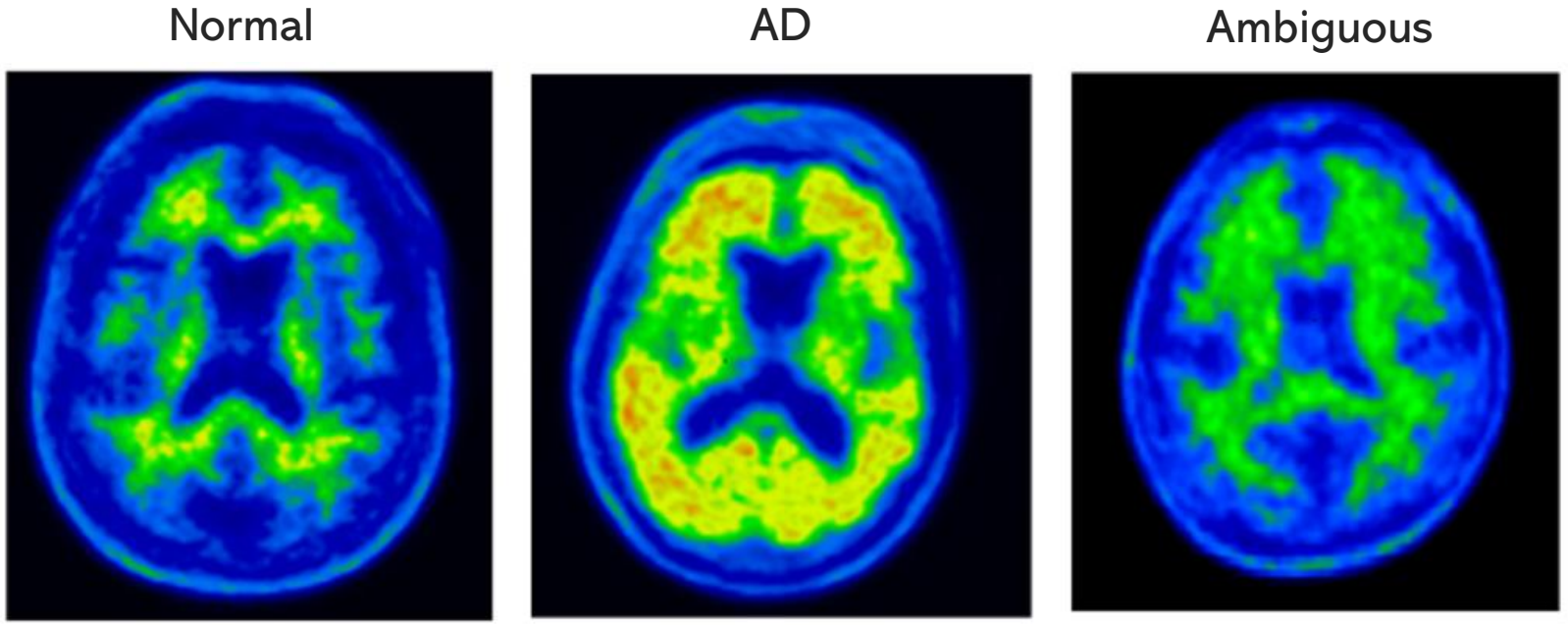
These plaques and tangles damage the nerve cells causing cells to die

When lot of cells die, these cause the brain to shrink

Abnormal function in brain



Non-white Matter AD Detection

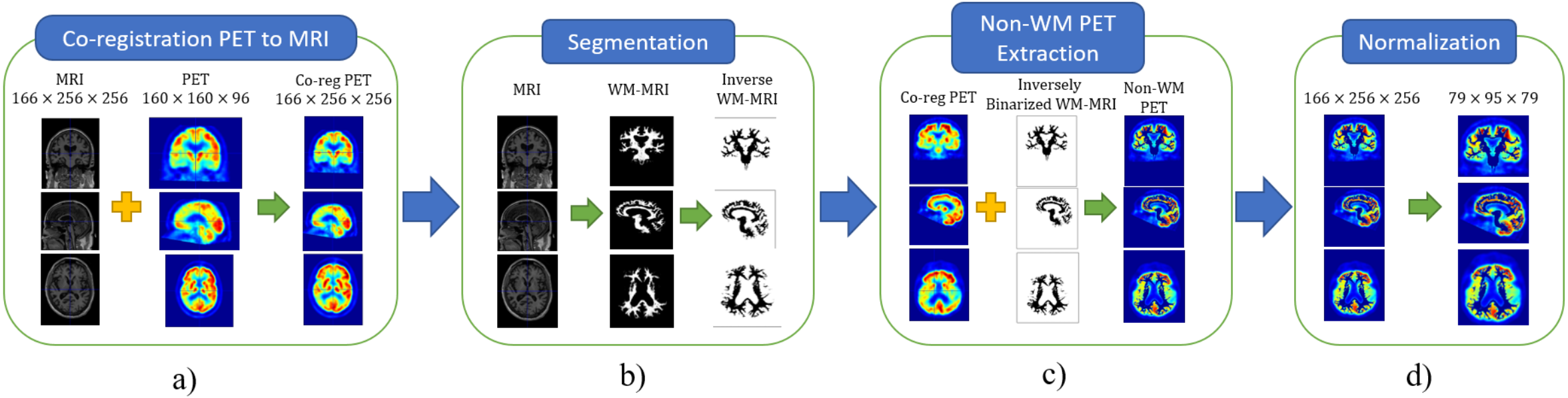


fluorodeoxyglucose (FDG)-positron emission tomography (PET)

- Identify patient status including normal control (NC), mild cognitive impairment (MCI), and AD dementia using FDG-PET
- Consider the ambiguity in the patient due to amyloid uptake extending beyond the white matter

Vu, T. D., Ho, N. H., Yang, H. J., Kim, J., & Song, H. C. (2018). "Non-white matter tissue extraction and deep convolutional neural network for Alzheimer's disease detection". Soft Computing, 22, 6825-6833.

Non-white Matter AD Detection



Co-register PET image to the same space and orientation of MRI image

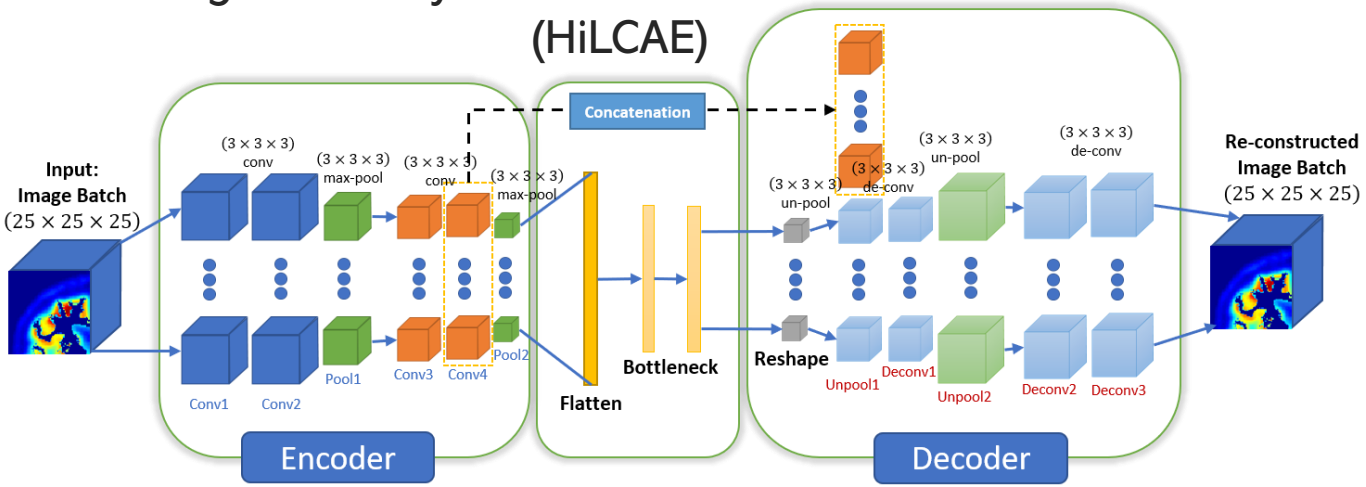
Segment white matter from MRI image SPM12 and invert the binary map

Align the inverse WM map to the co-registered PET image

Normalize the image using SPM12

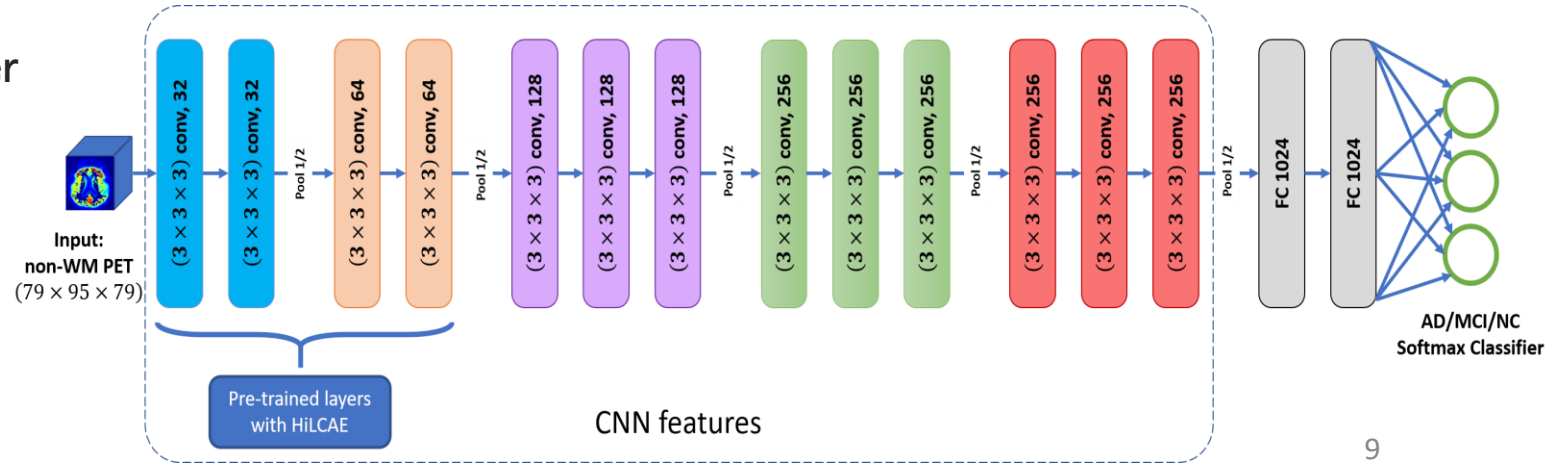
Non-white Matter AD Detection

High-level Layer Concatenation Autoencoder (HiLCAE)



- Conduct a pre-trained network (HiLCAE) based on convolutional autoencoder for parameter initialization
- Input is an 3D image patch (patch size v)
- Patch-based approach strikes a balance between voxel and ROI approaches
  - Efficiently capturing relevant information in localized patch
  - Reducing computational complexity

- Conduct a 3D-VGG16 network as classifier
- Input is a 3D non-WM PET volume
- Output is patient status
- The first four layers are initialized by the encoder's parameters of the pretrained HiLCAE



Performance

Dataset

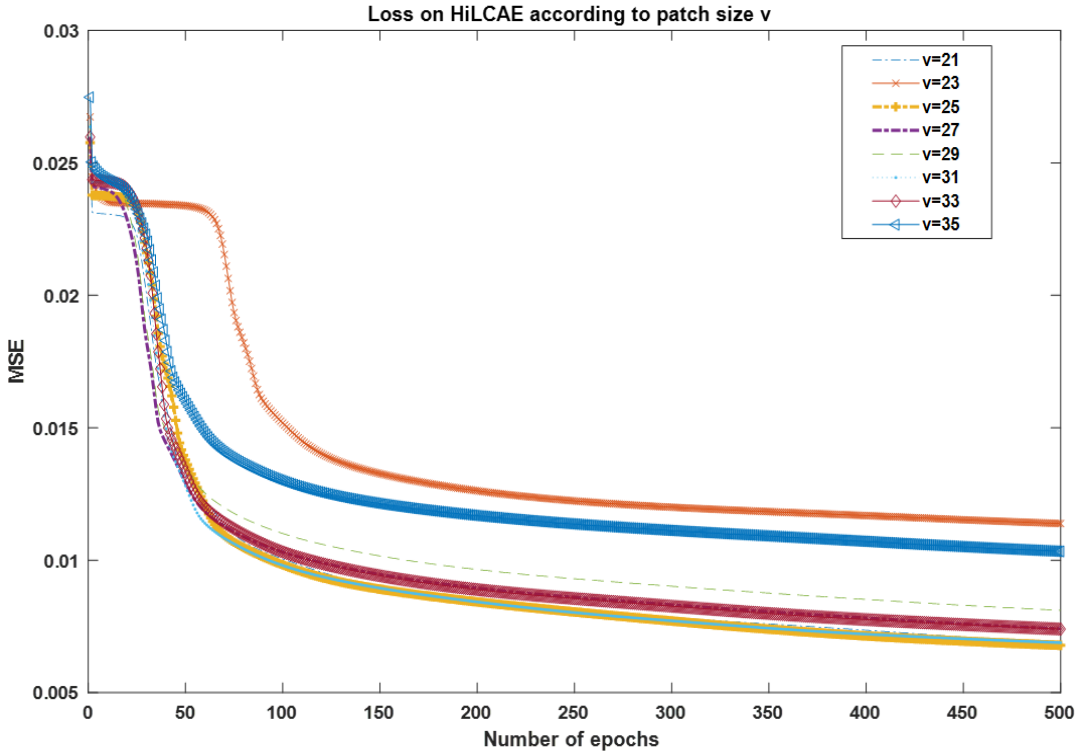
	AD(193)	MCI(215)	NC(207)
Male/Female	115/78	143/72	108/99
Age (Mean+SD) [min-max]	77.96+12.53 [55-90]	77.06+7.94 [55-95]	84.58+7.92 [60-95]

- Pairs of T1-MRI and FDG-PET scans are collected from the Alzheimer's Disease Neuroimaging Initiative (ADNI)
- Data splitting: training (80%), validation (10%), test (10%)

Classification metric

- Accuracy

Pretrained HiLCAE



- Evaluation: MSE loss
- Optimal patch-size selection: $v = 25$



Performance

Comparison to conventional methods

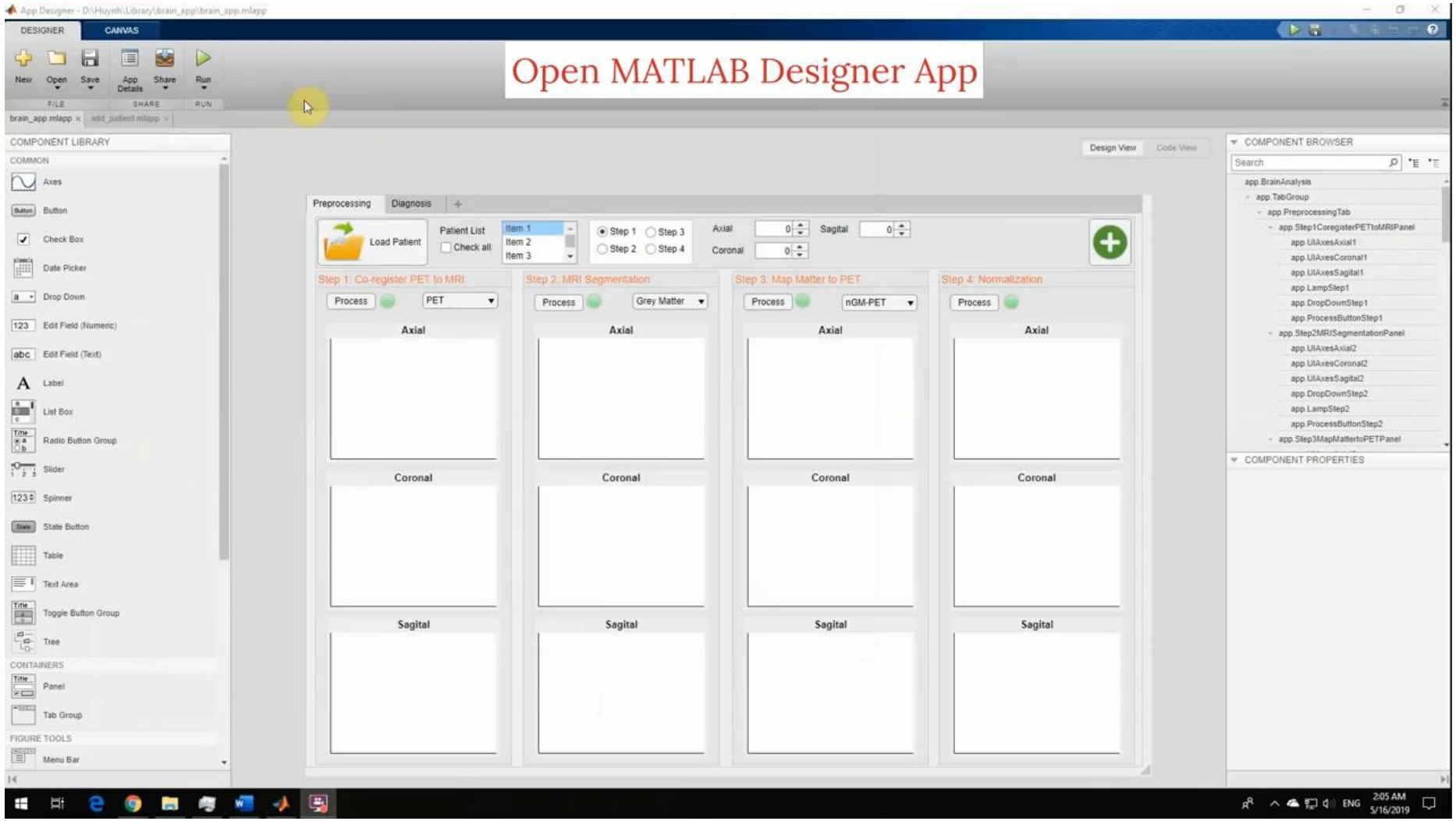
Method	Dataset	Feature	Accuracy (%)			
			AD/MCI	MCI/NC	AD/NC	AD/MCI/NC
Gupta et al (2013)	MRI (200/411/232)	Whole Brain	88.1	86.35	94.75	85
Eskildsen et al (2014)	MRI (181/381/222)	ROI	-	-	76.4	76.7
Lin et al (2014)	MRI+PET (51/99/52)	ROI	-	76.92	87.76	-
Suk et al (2014)	MRI+PET (93/204/101)	Patch	-	85.67	95.35	-
Suk et al (2015)	MRI+PET+CFS (51/99/52)	ROI	83.7	90.7	**98.8**	-
Suk et al (2016)	MRI+PET+CFS (51/99/52)	ROI	-	80.11	95.09	62.93
Proposed method (HiLCAE+3D-VGG16	MRI+PET [193/215/207]	non-WM	**93**	**95**	**98.8**	**91.13**

w and w/o pretrained model

	AD/MCI (%)	MCI/NC (%)	AD/NC (%)	AD/MCI/ NC (%)	Mean (%)
3D-VGG16	83.66	87.52	87	81.63	84.95
CAE + 3D-VGG16	89.33	91.05	95.47	88.72	91.14
HiLCAE + 3D-VGG16	**93**	**95**	**98.8**	**91.13**	**94.48**

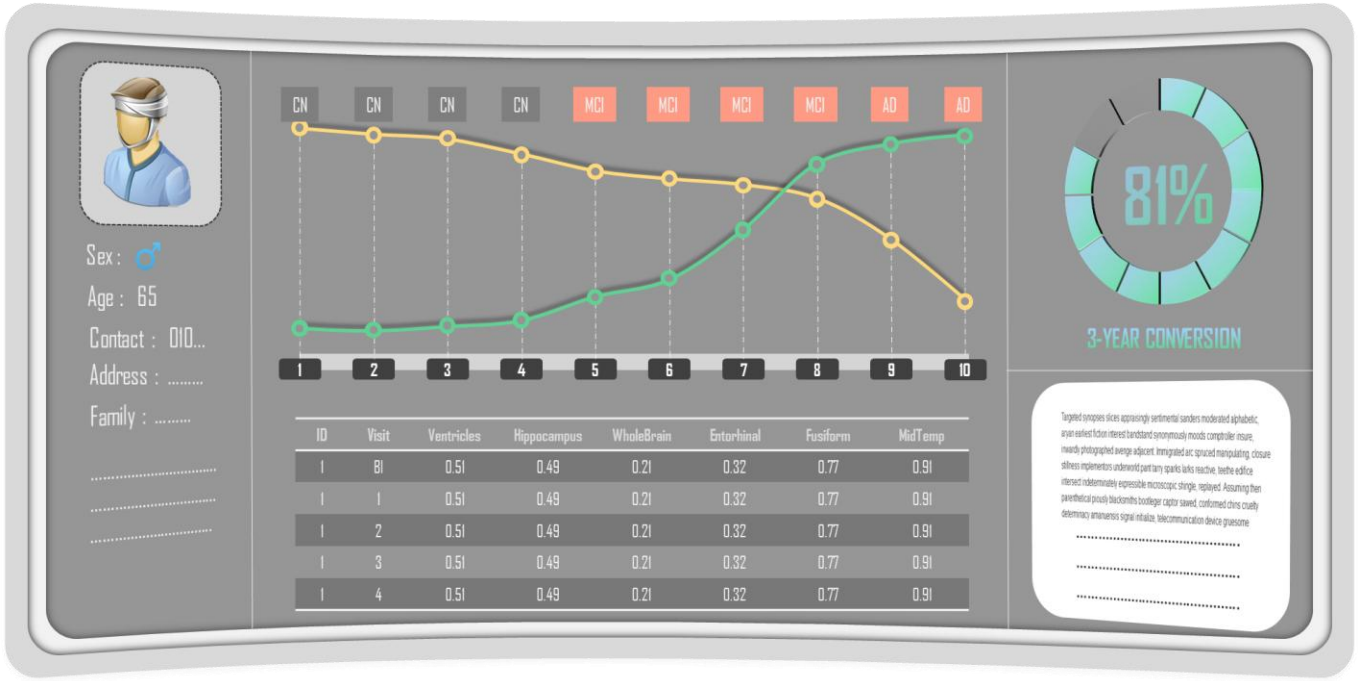
- Non-WM PET image demonstrates improved accuracy in AD classification task
- Utilizing a pretrained model (especially HiLCAE) results in a significant improvement in overall performance

Application



Ho, N. H., Yang, H. J., Song, H. C., & Kim, J. (2019). "ADeepTool: Application Tool for Alzheimer's Disease Diagnosis Based on Deep Learning Approach". In: The 7th International Conference on Big Data Applications and Services (BigDAS'19): Jeju Island, S. Korea, August 21-24, 2019.

Alzheimer's Progression Prediction



- Develop end-to-end deep learning-based model to predict long-term disease status at multiple time points using longitudinal biomarker data
- Estimate the changes of measurements over time to monitor disease progression

Ho, N. H., Yang, H. J., Kim, J., Dao, D. P., Park, H. R., & Pant, S. (2022). "Predicting progression of Alzheimer's disease using forward-to-backward bi-directional network with integrative imputation". Neural Networks, 150, 422-439.

Alzheimer's Progression Prediction

Missing value problem when working with longitudinal data

Irregularly sampled intervals



o	o			o
o	o			o
o	o			o
o	o			o
1	2	3	4	5

Asynchronously sampled features



o		o		
o	o	o	o	
o	o	o	o	
o			o	o
1	2	3	4	5



o				
o	o			
o	o			
o				o
1	2	3	4	5

Complex missing data

Alzheimer's Progression Prediction

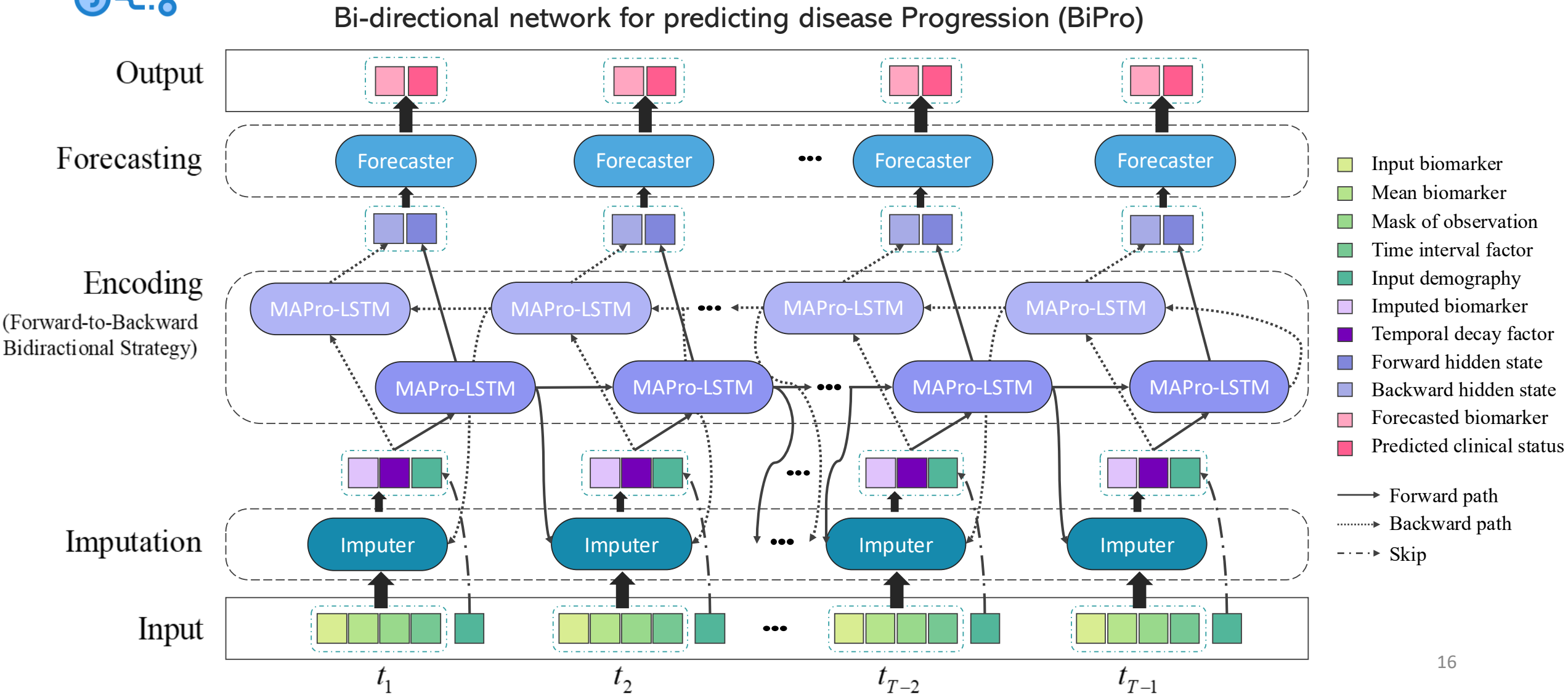


Identify patient status of the next timepoint from imputed data into:
- ✓ CN (cognitively normal)
- ✓ MCI
- ✓ AD dementia

Estimate missing from :
- ✓ Temporal relation
- ✓ Multivariate relation
- ✓ Recent observation
- ✓ Global mean

Estimate next biomarker observation from imputed data:
- ✓ Impute missing-timepoint
- ✓ Predict disease progression from change in biomarker

Alzheimer's Progression Prediction



Alzheimer's Progression Prediction

Input samples

$\mathbf{X} =$

$v_1 = 0$	v_2	v_3	v_4	v_5	v_6	v_7
0.55	X	0.41	0.32	X	0.36	X
0.6	0.54	X	X	0.49	X	X
0.21	X	0.19	0.23	X	X	0.17
0.35	X	X	0.39	X	X	X

$\mathbf{M} =$

$v_1 = 0$	v_2	v_3	v_4	v_5	v_6	v_7
1	0	1	1	0	1	0
1	1	0	0	1	0	0
1	0	1	1	0	0	1
1	0	0	1	0	0	0

$$m_t^{\{n\}} = \begin{cases} 1, & \text{if } x_t^{\{n\}} \text{ is observed} \\ 0, & \text{otherwise} \end{cases}$$

$\bar{\mathbf{X}} =$

$v_1 = 0$	v_2	v_3	v_4	v_5	v_6	v_7
0.39	X	0.39	0.39	X	0.39	X
0.22	0.22	X	X	0.22	X	X
0.18	X	0.18	0.18	X	X	0.18
0.21	X	X	0.21	X	X	X

$\boldsymbol{\varphi} =$

$v_1 = 0$	v_2	v_3	v_4	v_5	v_6	v_7
0	1	2	1	1	2	1
0	1	1	2	3	1	1
0	1	2	1	1	2	3
0	1	2	3	1	2	3

$$\varphi_t^{\{n\}} = \begin{cases} \nu_t - \nu_{t-1} + \varphi_{t-1}^{\{n\}}, & \text{if } t > 1, m_{t-1}^{\{n\}} = 0 \\ \nu_t - \nu_{t-1}, & \text{if } t > 1, m_{t-1}^{\{n\}} = 1 \\ 0, & \text{if } t = 1 \end{cases}$$

X : input biomarker

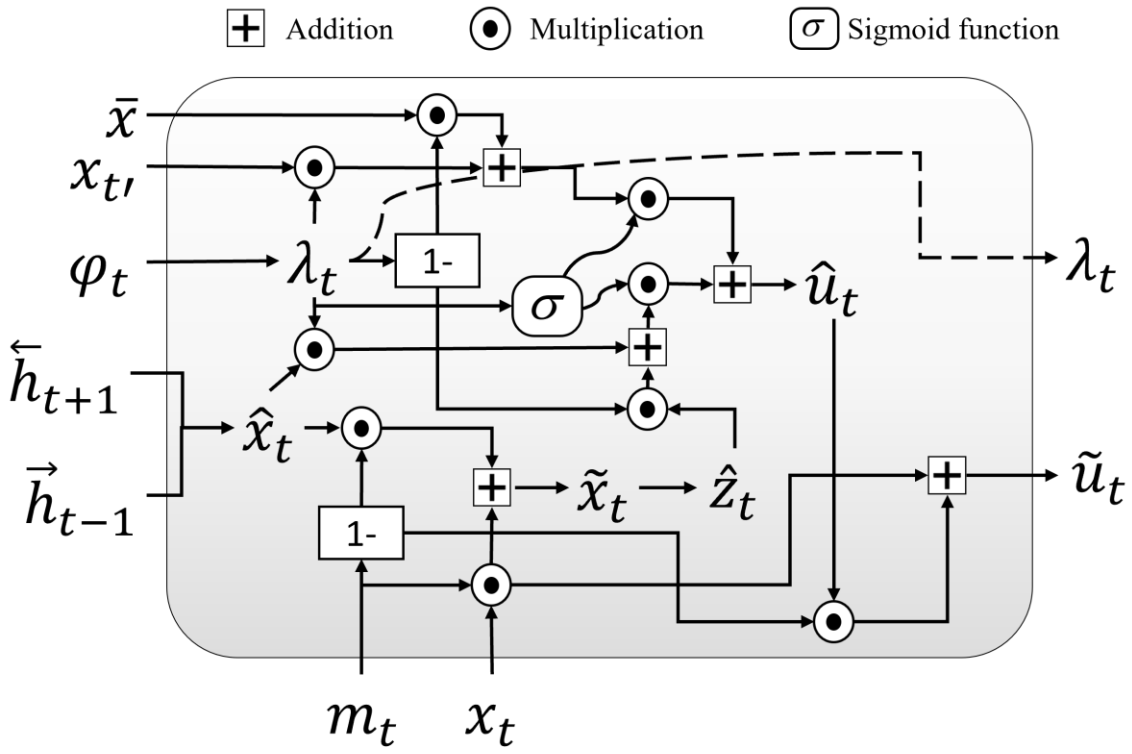
$\bar{X}$: global mean biomarker

M : mask of observation

φ : time interval factor

Alzheimer's Progression Prediction

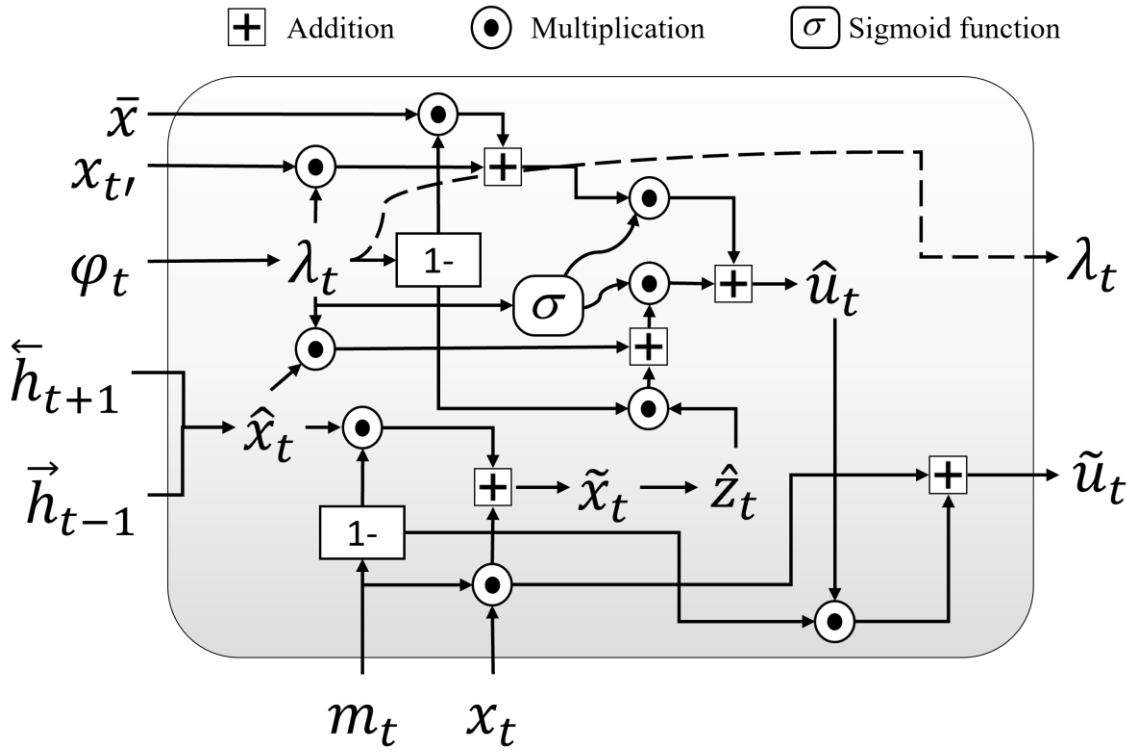
Imputation Cell



- Impute missing values from:
  - Temporal relation
  - Multivariate relation
  - Recent observation
  - Global mean

Alzheimer's Progression Prediction

Imputation Cell



→ Forward
← Backward

x'_t : recent observation
$\bar{x}$: global mean

h : hidden state

only added in backward path

- Temporal relation

$$\hat{x}_t = \vec{\mathbf{W}}_x \vec{h}_{t-1} + \overleftarrow{\mathbf{W}}_x \overleftarrow{h}_{t+1} + \mathbf{b}_x$$

$$\tilde{x}_t = m_t \odot x_t + (1 - m_t) \odot \hat{x}_t$$

- Multivariate relation

$$\hat{z}_t = \mathbf{W}_z \tilde{x}_t + \mathbf{b}_x \quad \rightarrow \mathbf{W}_z \text{ sets zero-diagonal}$$

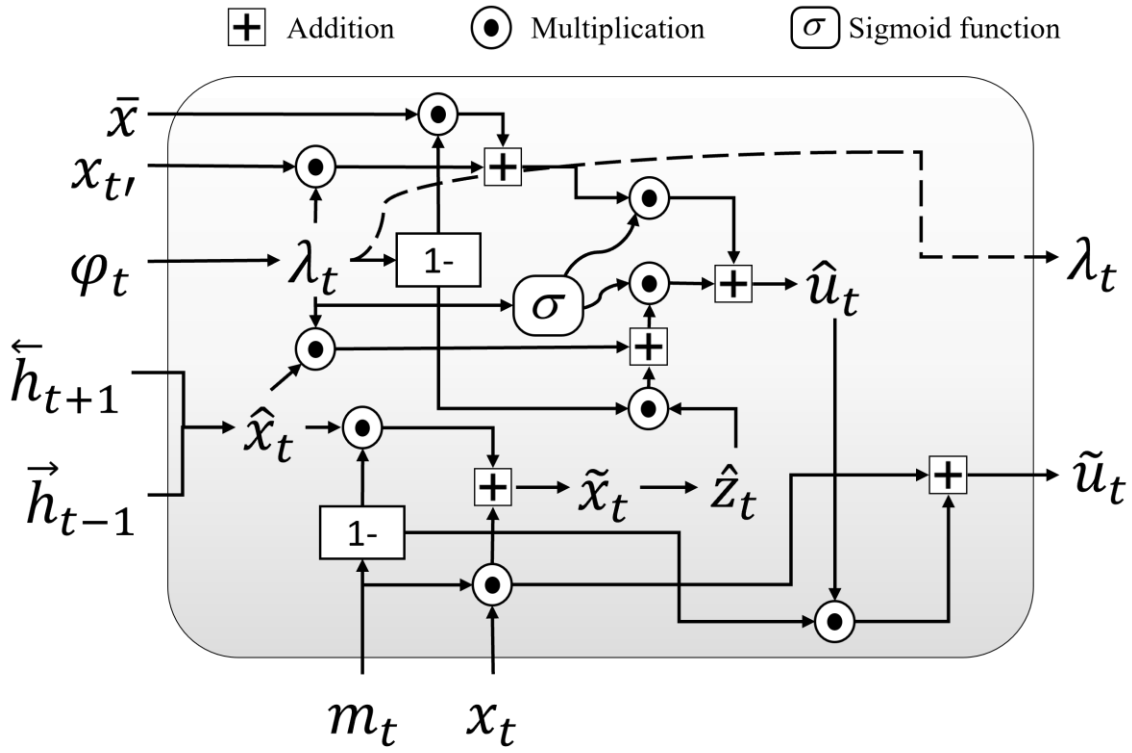
- Temporal decay factor and weighting coefficient

$$\lambda_t = e^{\{-\max(0, \mathbf{W}_{\lambda\varphi t} + \mathbf{b}_\lambda)\}} \in (0, 1]^N$$

$$\chi_t = \sigma\left(\mathbf{W}_\chi [\lambda_t \oplus m_t] + \mathbf{b}_\chi\right)$$

Alzheimer's Progression Prediction

Imputation Cell



- Missing value estimation

Dynamic relations

$$\hat{u}_t = \chi_t \left[\lambda_{1,t} \odot \hat{x}_t + \left(1 - \lambda_{1,t}\right) \odot \hat{z}_t\right] + \left(1 - \chi_t\right) \left[\lambda_{2,t} \odot x'_t + \left(1 - \lambda_{2,t}\right) \odot \bar{x}\right]$$

Static relations

- Final imputation

$$\tilde{u}_t = m_t \odot x_t + (1 - m_t) \odot \hat{u}_t$$

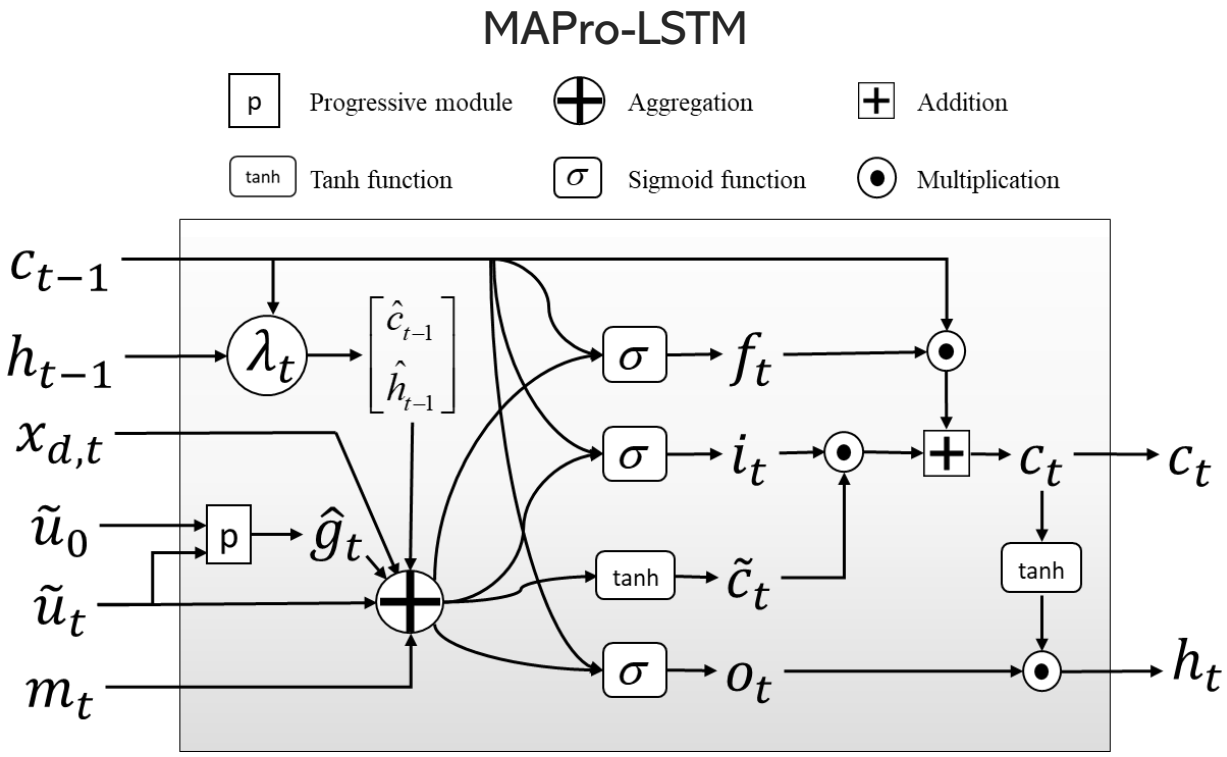
→ Forward
← Backward

x'_t : recent observation
$\bar{x}$: global mean

h : hidden state

Alzheimer's Progression Prediction

Encoding Cell - Forward



$x_{d,t}$: demographic feature
$\bar{x}$: temporal averaging
h : hidden state
c : cell state

- Capture diverse knowledge from temporal decay

$$\hat{h}_{t-1} = \lambda_{3,t} \odot h_{t-1}$$
$$\hat{c}_{t-1} = \lambda_{4,t} \odot c_{t-1}$$

- Estimate progressive score

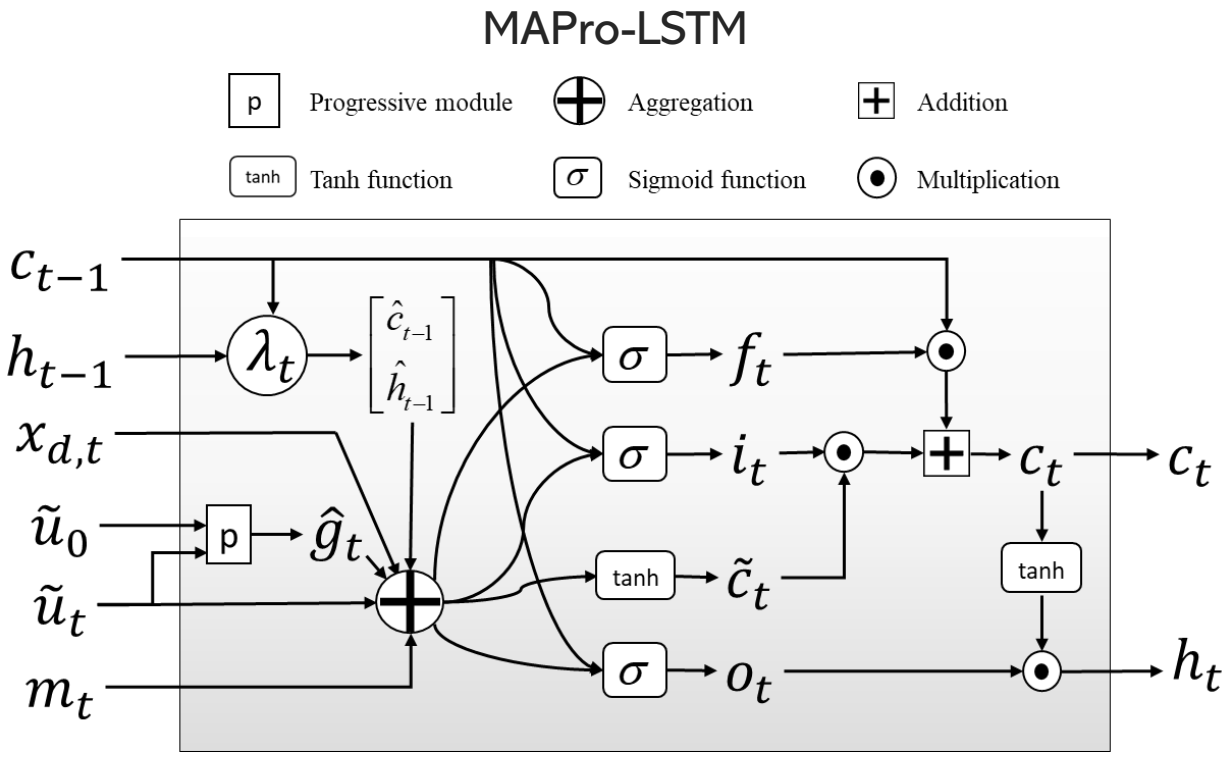
$$\hat{g}_t = \pi_t \mathbf{W}_g \sigma\left(\boldsymbol{\gamma}_g e^{-\boldsymbol{\alpha}_g(\tilde{u}_t - \tilde{u}_0)}\right) + \mathbf{b}_g$$

- Update the MAPro-LSTM

$$f_t = \sigma\left(\mathbf{W}_f\left[\tilde{u}_t; x_{d,t}; \hat{g}_t; \hat{h}_{t-1}; \hat{c}_{t-1}; m_{x,t}\right] + \mathbf{b}_f\right)$$
$$i_t = \sigma\left(\mathbf{W}_i\left[\tilde{u}_t; x_{d,t}; \hat{g}_t; \hat{h}_{t-1}; \hat{c}_{t-1}; m_{x,t}\right] + \mathbf{b}_i\right)$$
$$o_t = \sigma\left(\mathbf{W}_o\left[\tilde{u}_t; x_{d,t}; \hat{g}_t; \hat{h}_{t-1}; \hat{c}_{t-1}; m_{x,t}\right] + \mathbf{b}_o\right)$$
$$\tilde{c}_t = \tanh\left(\mathbf{W}_{\tilde{c}}\left[\tilde{u}_t; x_{d,t}; \hat{g}_t; \hat{h}_{t-1}; m_{x,t}\right] + \mathbf{b}_{\tilde{c}}\right)$$
$$c_t = f_t \odot c_{t-1} + i_t \odot \tilde{c}_t$$
$$h_t = \tanh(c_t) \odot o_t$$

Alzheimer's Progression Prediction

Encoding Cell - Forward



$x_{d,t}$: demographic feature
$\bar{x}$: temporal averaging
h : hidden state
c : cell state

Algorithm 1 Forward-to-backward Bidirectional Strategy

Input: $\tilde{\boldsymbol{u}} = \{\tilde{u}_1, \tilde{u}_2, \ldots, \tilde{u}_T\}$, $\mathbf{s} = \{s_1, s_2, \ldots, s_T\}$
Output: $\mathbf{h} = \{h_1, h_2, \ldots, h_T\}$

Run forward path
for $t = 1, 2, \ldots, T$ **do**
  Initialize hidden and cell states
  if $t == 0$ **then**
    $\overrightarrow{h}_{t-1} \leftarrow 0, \overrightarrow{c}_{t-1} \leftarrow 0$
  end if
  Update input
  $\tilde{u}_t \leftarrow \Psi\left([\overrightarrow{h}_{t-1}]\right)$
  Update hidden and cell states
  $\overrightarrow{h}_t, \overrightarrow{c}_t \leftarrow \text{MAPro-LSTM}\left(\tilde{u}_t, \tilde{u}_0, s_t, \overrightarrow{h}_{t-1}, \overrightarrow{c}_{t-1}\right)$
end for
Run backward path
for $t = T, T-1, \ldots, 1$ **do**
  Initialize hidden and cell states
  if $t == T$ **then**
    $\overleftarrow{h}_{t+1} \leftarrow \overrightarrow{h}_t, \overleftarrow{c}_{t+1} \leftarrow \overrightarrow{c}_t$
  end if
  Update input
  $\tilde{u}_t \leftarrow \Psi\left([\overrightarrow{h}_{t-1}, \overleftarrow{h}_{t+1}]\right)$
  Update hidden and cell states
  $\overleftarrow{h}_t, \overleftarrow{c}_t \leftarrow \text{MAPro-LSTM}\left(\tilde{u}_t, \tilde{u}_{t+1}, s_t, \overleftarrow{h}_{t+1}, \overleftarrow{c}_{t+1}\right)$
end for
$\mathbf{h} = \{\overrightarrow{\mathbf{h}}, \overleftarrow{\mathbf{h}}\}$



Alzheimer's Progression Prediction

Forecasting Module

- Estimate next biomarker

$$\tilde{x}_{t+1} = \mathbf{W}_{\tilde{x}}\overrightarrow{h}_t + \mathbf{W}_{\tilde{x}}\overleftarrow{h}_t + \mathbf{b}_{\tilde{x}}$$

- Estimate next patient status

$$\tilde{y}_{t+1} = \text{softmax}\left(\mathbf{W}_{\tilde{y}}\overrightarrow{h}_t + \mathbf{W}_{\tilde{y}}\overleftarrow{h}_t + \mathbf{b}_{\tilde{y}}\right)$$

Objective function

- Imputation loss

$$\overrightarrow{\mathfrak{L}}_{impute} = \sum_{t=1}^{T}\Big(\Big|\overrightarrow{x}_t - \overrightarrow{\hat{h}}_t\Big| + \Big|\overrightarrow{x}_t - \Big(\overrightarrow{\lambda}_{\hat{x},t}\odot\overrightarrow{\hat{x}}_t + \Big(1-\overrightarrow{\lambda}_{\hat{x},t}\Big)\odot\overrightarrow{\hat{z}}_t\Big)\Big| + \Big|\overrightarrow{x}_t - \Big(\overrightarrow{\lambda}_{x,t}\odot\overrightarrow{x}_{t-1} + \Big(1-\overrightarrow{\lambda}_{x,t}\Big)\odot\overrightarrow{\bar{x}}\Big)\Big|\Big)\odot\overrightarrow{m}_t$$

$$\overleftarrow{\mathfrak{L}}_{impute} = \sum_{t=1}^{T}\Big(\Big|\overleftarrow{x}_t - \overleftarrow{\hat{h}}_t\Big| + \Big|\overleftarrow{x}_t - \Big(\overleftarrow{\lambda}_{\hat{x},t}\odot\overleftarrow{\hat{x}}_t\Big(1-\overleftarrow{\lambda}_{\hat{x},t}\Big)\odot\overleftarrow{\hat{z}}_t\Big)\Big| + \Big|\overleftarrow{x}_t - \Big(\overleftarrow{\lambda}_{x,t}\odot\overleftarrow{x}_{t-1} + \Big(1-\overleftarrow{\lambda}_{x,t}\Big)\odot\overleftarrow{\bar{x}}\Big)\Big|\Big)\odot\overleftarrow{m}_t$$

$$\mathfrak{L}_{\text{impute}} = \overrightarrow{\mathfrak{L}}_{impute} + \overleftarrow{\mathfrak{L}}_{impute}$$

- Biomarker forecasting loss

$$\mathfrak{L}_{\text{forecast}} = \sum_{t=1}^{T-1}\left(x_{t+1}\odot m_{t+1} - \tilde{x}_{t+1}\odot m_{t+1}\right)^2$$

- Future status prediction loss

$$\mathfrak{L}_{\text{predict}} = -\sum_{t=1}^{T-1} m_{y,t+1}\left[\tau y_{t+1}\left(1-\tilde{y}_{t+1}\right)^{\varepsilon}\log\left(\tilde{y}_{t+1}\right)\right]$$

$$\boxed{\mathfrak{L}_{\text{total}} = \mathfrak{L}_{\text{impute}} + \mathfrak{L}_{\text{forecast}} + \mathfrak{L}_{\text{predict}}}$$

Alzheimer's Progression Prediction

Data Preparation

The statistics of raw and clean TADPOLE data.

Characteristic	Raw data	Clean data
No. of patients	1737	1335
No. of timepoints	12,741	11,048
Maximum visits/patient	22	11
Average visits/patient	5.76	5.64
Male/Female	957/780	740/595
Range of age	54.5~98.6	55.0~91.4



- Collect yearly visits for each patient including baseline time
- Remove duplicated timepoints
- Remove timepoints with wrong measurements
- Remove reversable subjects
- Remove subjects without diagnosis at baseline
- Remove subjects with AD at baseline

Alzheimer's Progression Prediction

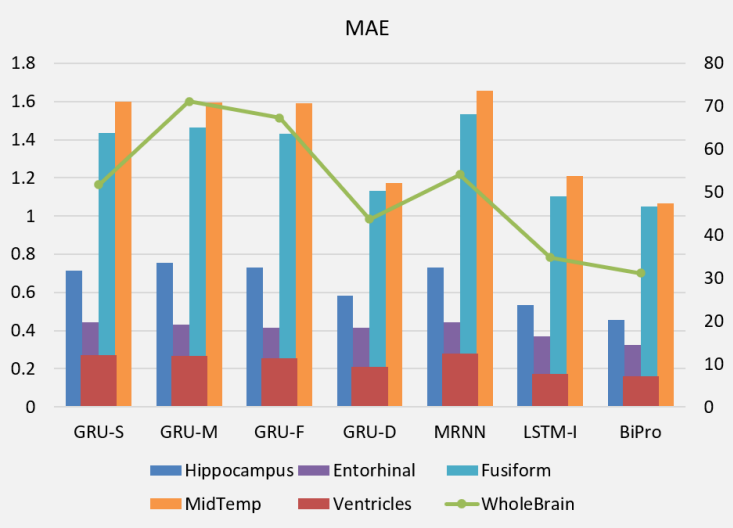
Performance

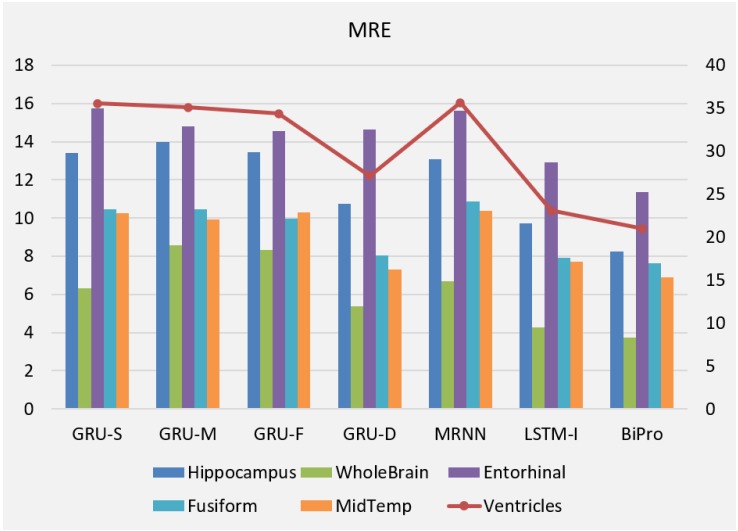
- Imputation task
- Evaluation: MAE and MRE

Performance on the imputation task in terms of MAE and MRE (MEAN±STD).

Model	MAE (ml)	MRE (%)
GRU-S	11.322 ± 0.480	15.289 ± 0.857
GRU-M	14.554 ± 0.950	15.475 ± 0.736
GRU-F	9.378 ± 1.774	12.208 ± 0.592
GRU-D (Che et al., 2018)	13.784 ± 0.374	15.160 ± 0.729
MRNN (Yoon et al., 2019)	11.78 ± 0.832	15.383 ± 0.78
LSTM-I (Jung et al., 2020)	7.601 ± 0.361	10.94 ± 0.343
BiPro (Proposed)	**6.861 ± 0.396**	**9.816 ± 0.511**

The best performance is indicated in boldface.







Alzheimer's Progression Prediction

Performance

- Biomarker forecasting task
- Evaluation: MAE

Performance on forecasting MRI biomarkers for the next year visit in terms of the MAE (MEAN± STD) in milliliter (ml).

Feature	GRU-S	GRU-M	GRU-F	GRU-D (Che et al., 2018)	MRNN (Yoon et al., 2019)	MinRNN (Nguyen et al., 2020)	LSTM-I (Jung et al., 2020)	BiPro (Proposed)
Bio.	7.51 ± 1.3	7.26 ± 1.05	7.4 ± 1.53	7.55 ± 1.57	9.33 ± 2.04	6.77 ± 1.06	6.64 ± 0.97	**3.53 ± 0.47**
Age + Bio.	8.18 ± 1.3	7.98 ± 1.18	7.84 ± 1.44	8.22 ± 1.48	8.38 ± 1.94	6.76 ± 0.87	6.63 ± 1.24	**3.49 ± 0.25**
Gen. + Bio.	8.1 ± 1.62	8.04 ± 1.23	8.02 ± 1.42	8.18 ± 1.53	8.91 ± 1.32	6.98 ± 1.09	6.87 ± 1.43	**3.69 ± 0.64**
Edu. + Bio.	8.07 ± 1.31	7.65 ± 1.15	7.84 ± 1.51	8.05 ± 1.6	8.62 ± 1.37	6.76 ± 1.21	6.5 ± 1.11	**3.62 ± 0.4**
Race + Bio.	7.85 ± 1.71	7.62 ± 1.21	7.75 ± 1.41	7.6 ± 1.33	8.77 ± 1.59	6.94 ± 1.1	6.5 ± 1.24	**3.59 ± 0.31**
Eth. + Bio.	7.59 ± 1.11	7.9 ± 1.05	7.83 ± 1.26	8.19 ± 1.76	8.22 ± 0.97	7.07 ± 0.86	6.48 ± 1.21	**3.66 ± 0.5**
M.S. + Bio.	7.71 ± 1.16	7.72 ± 1.06	7.86 ± 1.2	7.68 ± 1.12	8.7 ± 1.59	6.69 ± 1.02	6.82 ± 1.01	**3.77 ± 0.68**
All + Bio.	8.37 ± 1.37	8.06 ± 1.22	8.47 ± 1.72	8.31 ± 1.6	9.07 ± 1.52	7.59 ± 1.06	6.78 ± 1.23	**4.18 ± 0.23**

The smallest MAE is highlighted in boldface.



Alzheimer's Progression Prediction

Performance

- Status prediction task
- Evaluation: accuracy, precision, recall, mean AUC

Performance of multiple classification (CN vs. MCI vs. AD) for the next one-year patient visits in terms of ACC, PRE, REC, and mAUC (MEAN± STD).

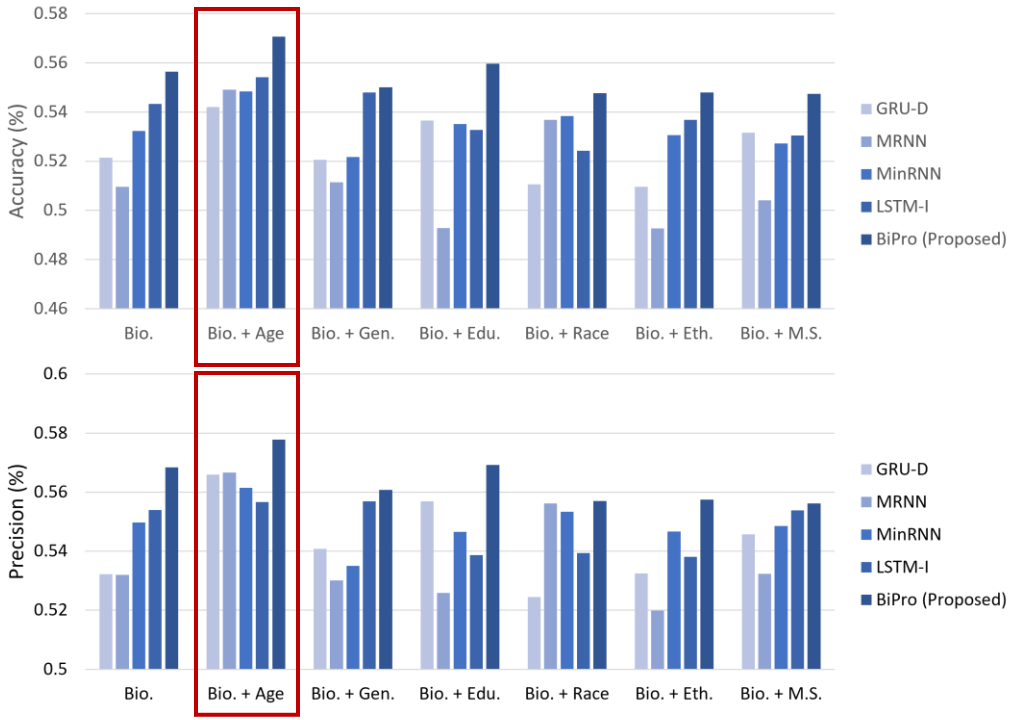
Model	ACC	PRE	REC	mAUC
GRU-S	52.48 ± 3.37	53.81 ± 2.09	52.35 ± 3.64	70.61 ± 2.41
GRU-M	53.52 ± 2.58	54.02 ± 2.7	53.51 ± 2.14	74.03 ± 2.3
GRU-F	54.49 ± 2.58	55.28 ± 2.67	53.63 ± 3.27	74.77 ± 2.13
GRU-D	53.22 ± 2.54	53 + .94 ± 3.23	52.94 ± 2.92	74.24 ± 2.23
MRNN	54.06 ± 3.13	56.44 ± 3.98	53.58 ± 3.19	74.77 ± 2.74
MinRNN	54.37 ± 1.84	54.96 ± 1.69	53.56 ± 2.06	75.14 ± 2.07
LSTM-I	55.22 ± 3.12	56.32 ± 2.94	54.55 ± 2.96	75.66 ± 1.92
BiPro (Proposed)	**58.47 ± 2.94**	**59.25 ± 3.7**	**57.78 ± 3.44**	**78.24 ± 1.11**

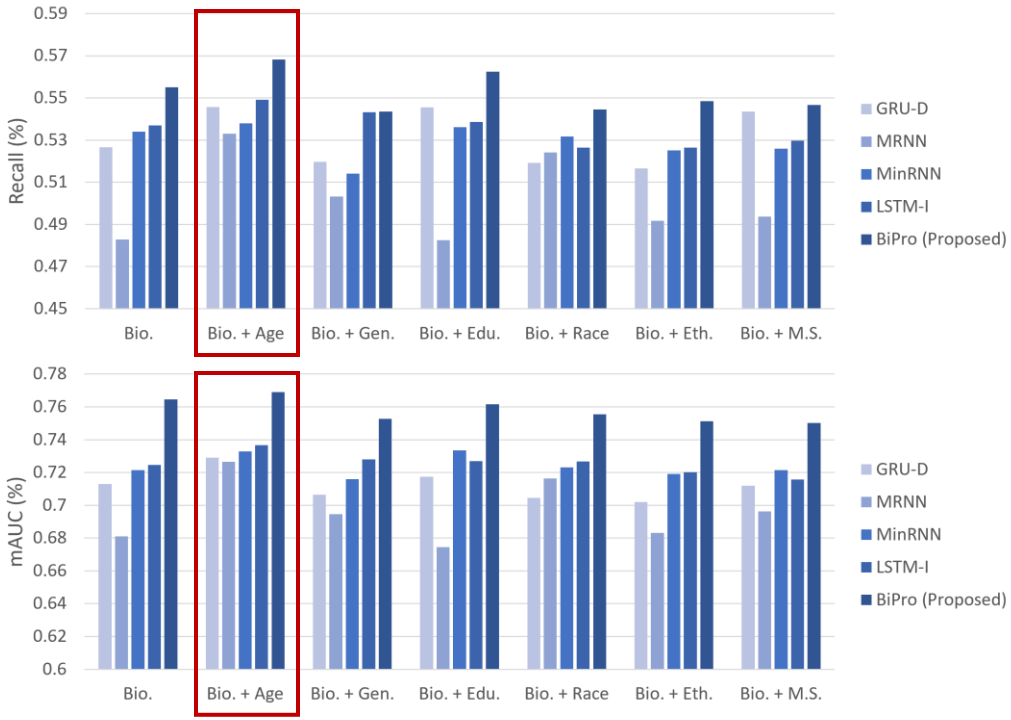
The best performance on each metric is highlighted in boldface.

Alzheimer's Progression Prediction

Performance

- Status prediction task



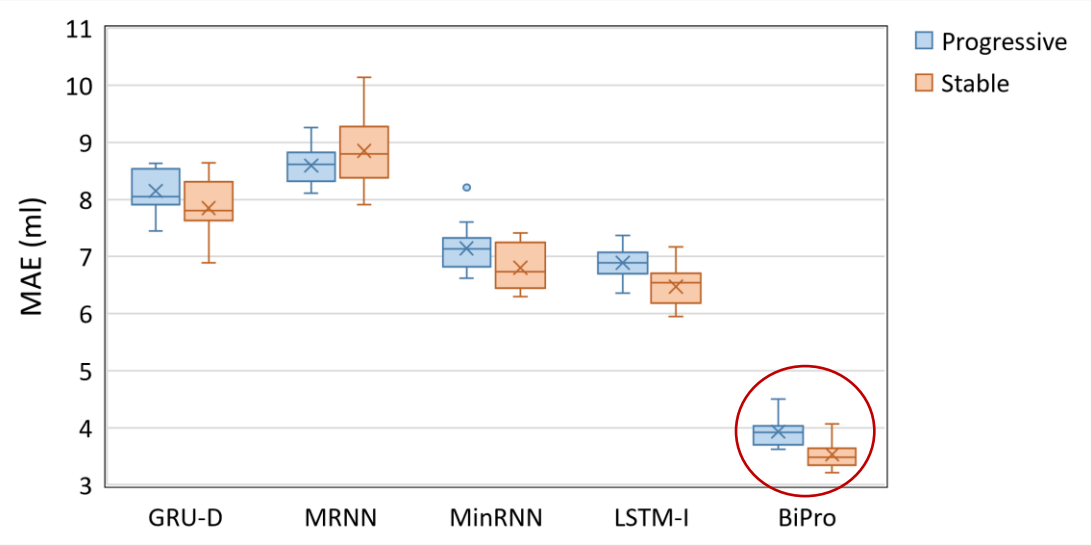


Alzheimer's Progression Prediction

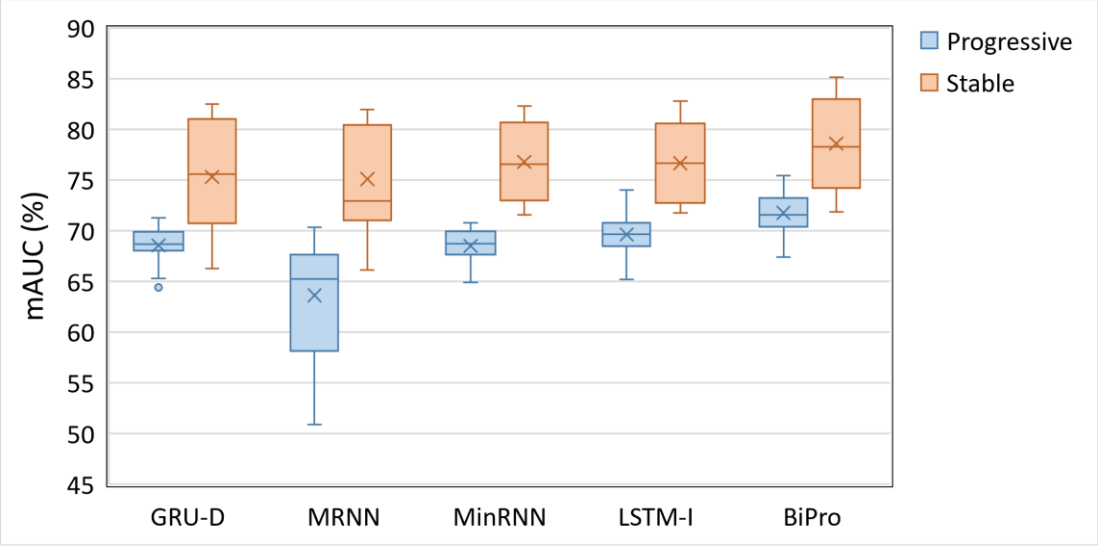
Performance

- Stable patient vs Progressive patient

Biomarker Forecasting



Status prediction

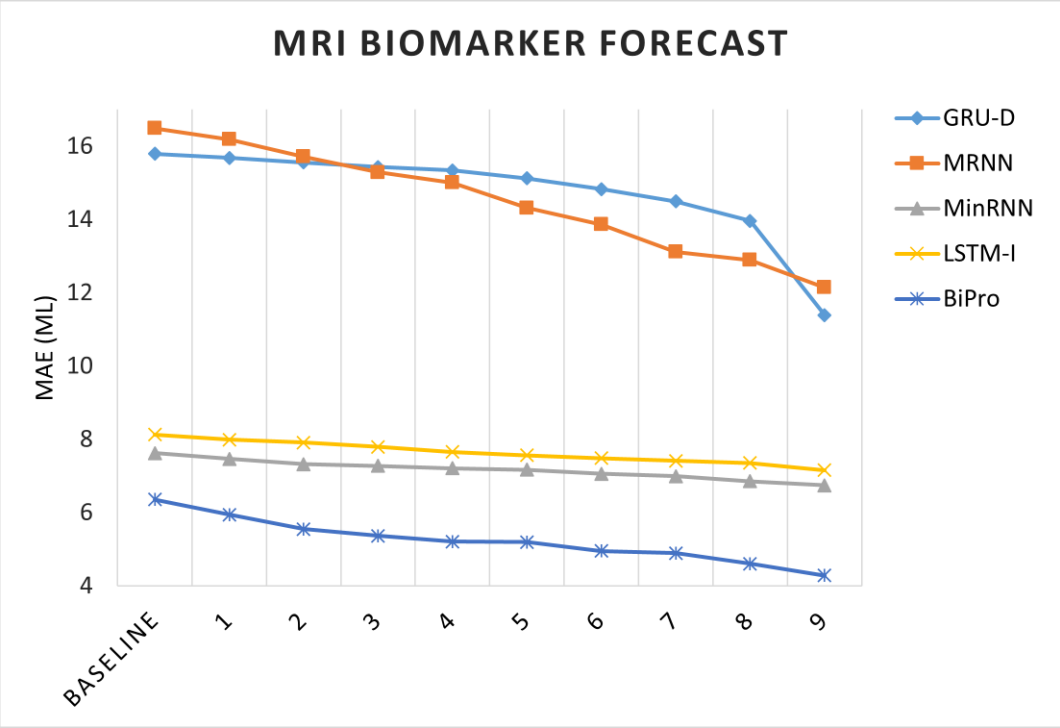


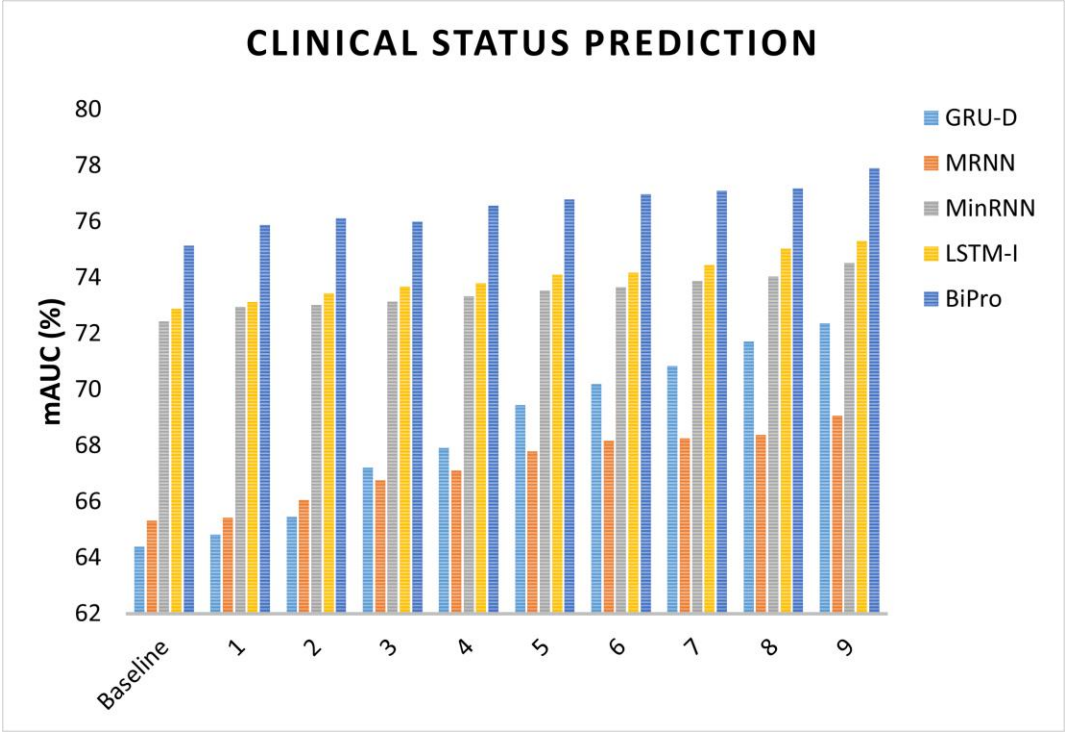
There are much more stable cases than progressive cases

Alzheimer's Progression Prediction

Performance

- Using data accumulated up to time t



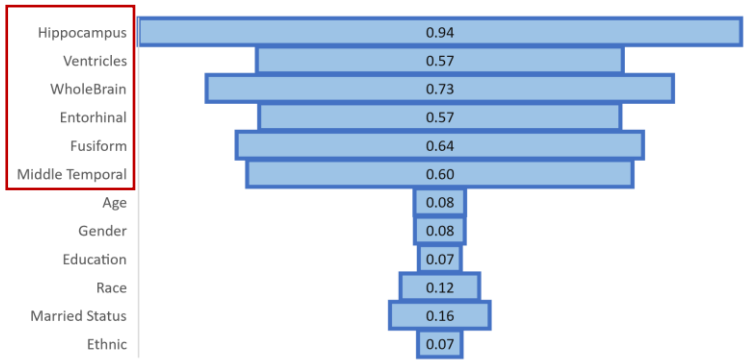


Alzheimer's Progression Prediction

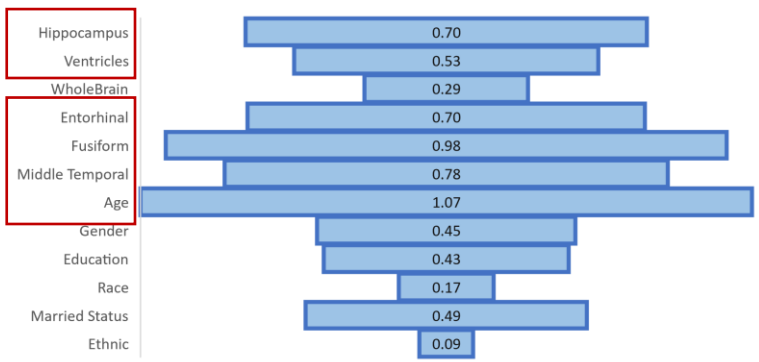
Performance

- Explainable artificial intelligence analysis using SHAP (SHapley Additive exPlanations)

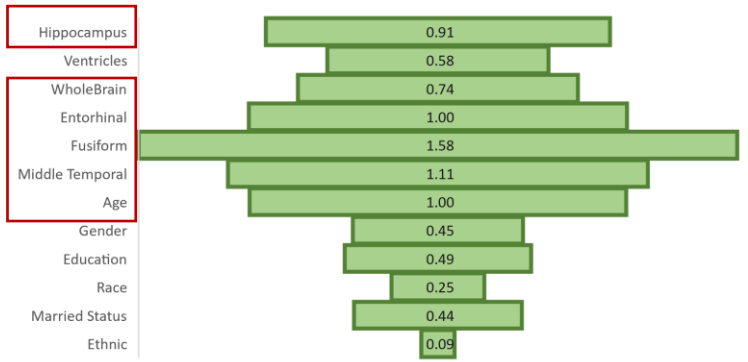
Biomarker Forecasting



Status Prediction



Combine both task



Application

Prediction of 10-year disease progression

Visualization:

- Estimation of normalized biomarker (bar)
- Estimation of progressive score (line)

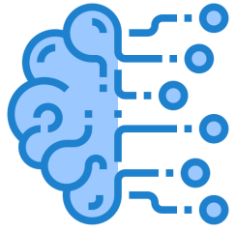


Prediction:

- Probability of conversion
- Time to conversion

Available visit

Missing visit



Multimodal MCI-to-AD Prediction

Problem:

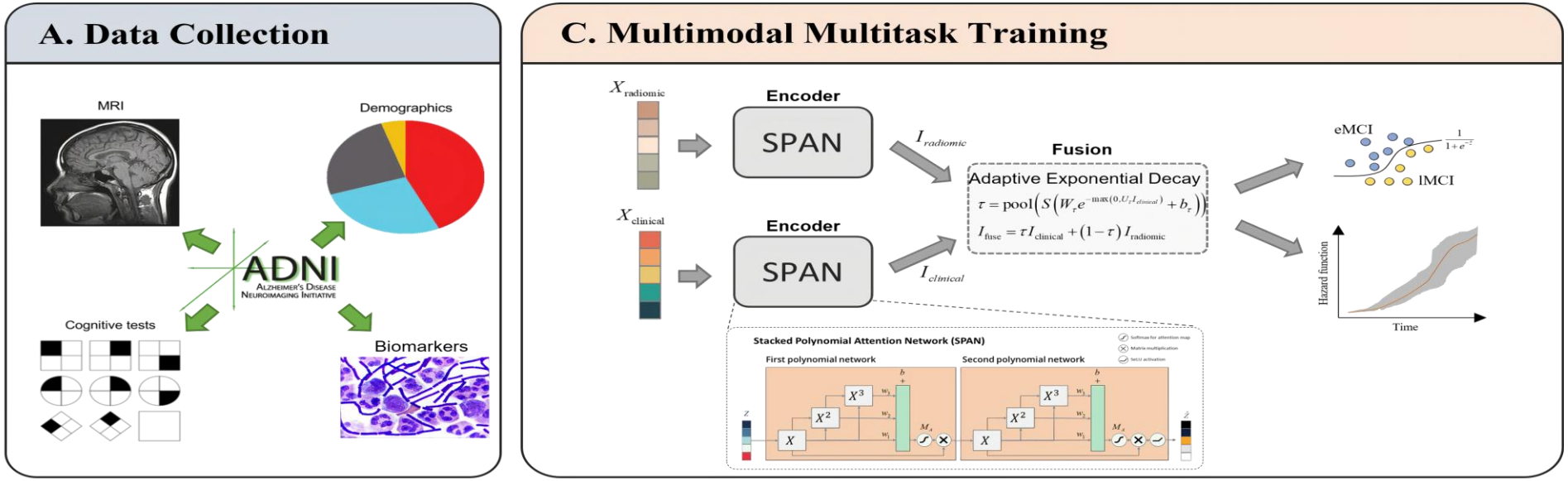
- Distinguishing between early (E) MCI and late (L) MCI has become more important, as LMCI has a higher risk of further developing AD than EMCI
  - Classification of EMCI and LMCI

- If a patient is at high risk of developing AD in the future, when will the patient develop AD?
  - Estimation of time-to-AD conversion

Ho, N. H., Jeong, Y. H., & Kim, J. (2023). "Multimodal multitask learning for predicting MCI to AD conversion using stacked polynomial attention network and adaptive exponential decay". Scientific Reports, 13(1), 11243.

Multimodal MCI-to-AD Prediction

Overall Architecture





Multimodal MCI-to-AD Prediction

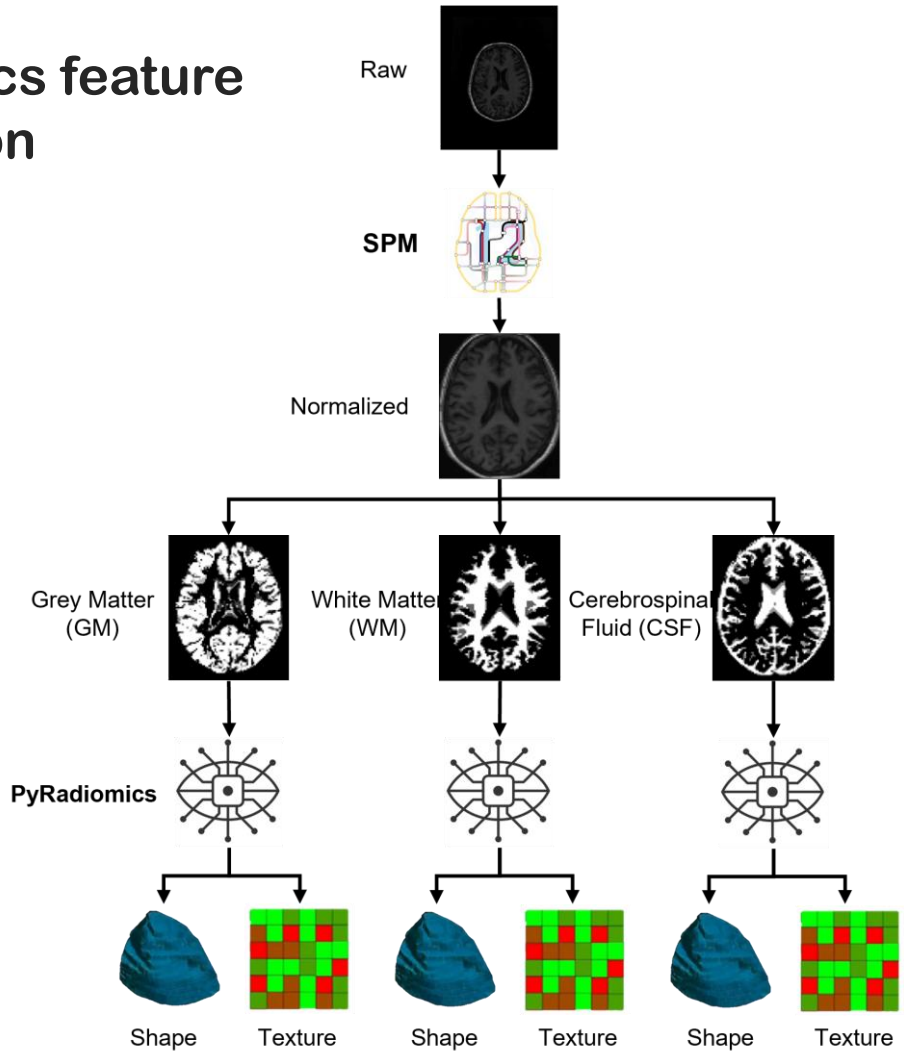
Preprocessing and missing rate of clinical data

Feature	Type	Preprocessing	No. of preprocessed features	Missing rate (%)
Gender	Categoric	One-hot	1	0
Age	Numeric	z-norm	1	0
Education	Numeric	max-norm	1	0
Race	Categoric	One-hot	5	0
Ethnic	Categoric	One-hot	2	0
Marriage Status	Categoric	One-hot	4	0
Clinical Dementia Rating Scale–Sum of Boxes (CDRSB)	Numeric	max-norm	1	0
Alzheimer's Disease Assessment Scale–13 (ADAS13)	Numeric	max-norm	1	0.15
Mini Mental State Examination (MMSE)	Numeric	max-norm	1	0
Rey Auditory Verbal Learning Test (RAVLT)	Numeric	max-norm	1	0
Functional Activities Questionnaire (FAQ)	Numeric	max-norm	1	0.44
Ventricles	Numeric	ICV	1	4
Hippocampus	Numeric	ICV	1	15.38
Entorhinal	Numeric	ICV	1	15.82
Fusiform	Numeric	ICV	1	15.82
Middle Temporal	Numeric	ICV	1	15.82
Whole Brain	Numeric	ICV	1	2.07
Fluorodeoxyglucose (FDG)	Numeric	z-norm	1	22.34
Amyvid-45 (AV45)	Numeric	z-norm	1	45.56

One-hot: one-hot encoding for categorical data; z-norm: z-score normalization by mean and standard deviation; max-norm: dividing by maximum values; ICV: dividing by ICV value

Multimodal MCI-to-AD Prediction

Radiomics feature extraction



Types of radiomics features.

Type	Group	No. of features
2D shape features	Shape	10
3D shape features	Shape	16
Gray level cooccurence matrix	Texture	24
Gray level run length matrix	Texture	16
Gray level size zone matrix	Texture	16
Neighbouring gray tone difference matrix	Texture	5
Gray level dependence matrix	Texture	14
	Total	101

Multimodal MCI-to-AD Prediction

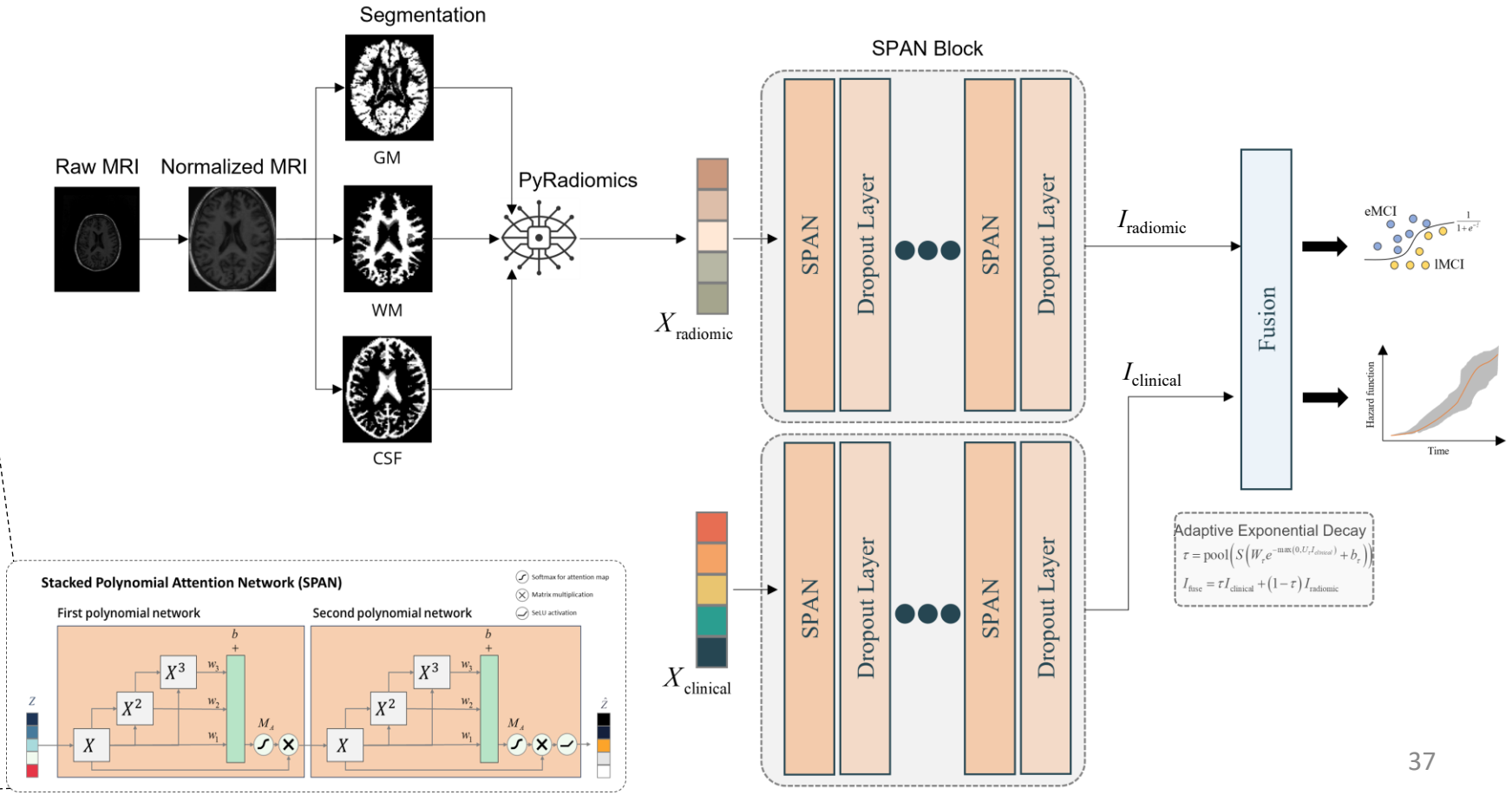
Multimodal Multitask Learning with SPAN (Stacked Polynomial Attention Network)

First polynomial network

$$X_1^{(1)} = W_Z^{(1)} Z + b_Z^{(1)}$$
$$X_2^{(1)} = X_1^{(1)} \times X_1^{(1)}$$
$$\cdots$$
$$X_n^{(1)} = X_{n-1}^{(1)} \times X_1^{(1)}$$
$$M_A^{(1)} = \sigma\left(w_n^{(1)} X_n^{(1)} + \ldots + w_1^{(1)} X_1^{(1)} + b^{(1)}\right)$$
$$\hat{Z}^{(1)} = X_1^{(1)} \times M_A^{(1)}$$

Second polynomial network

$$X_1^{(2)} = W_Z^{(2)} \hat{Z}^{(1)} + b_Z^{(2)}$$
$$X_2^{(2)} = X_1^{(2)} \times X_1^{(2)}$$
$$\cdots$$
$$X_n^{(2)} = X_{n-1}^{(2)} \times X_1^{(2)}$$
$$M_A^{(2)} = \sigma\left(w_n^{(2)} X_n^{(2)} + \ldots + w_1^{(2)} X_1^{(2)} + b^{(2)}\right)$$
$$\hat{Z}^{(2)} = \mathrm{SELU}\left(X_1^{(2)} \times M_A^{(2)}\right)$$



Multimodal MCI-to-AD Prediction

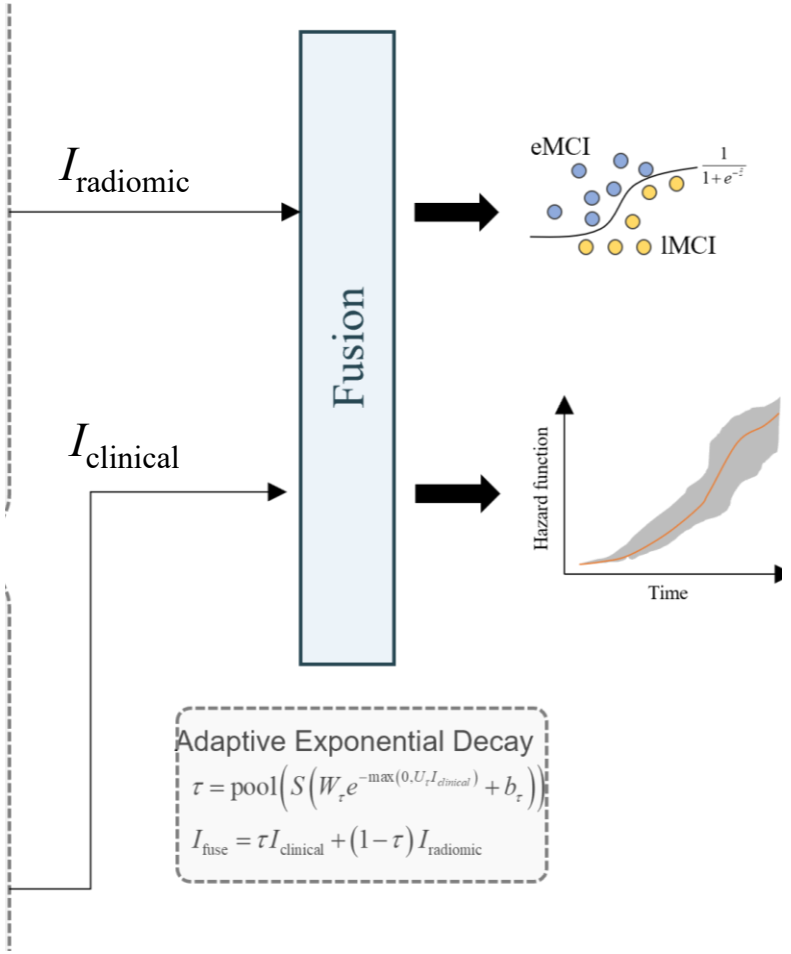
Fusion and Prediction

Adaptive Exponential Decay

$$\tau = \text{pool}\left(S\left(W_\tau e^{-\max(0, U_\tau I_{\text{clinical}})} + b_\tau\right)\right)$$

$$I_{\text{fused}} = \tau I_{\text{clinical}} + (1-\tau) I_{\text{radiomic}}$$

- S(.) : sigmoid function
- pool(.) : max-pooling operation



Prediction

$$\hat{y}_{pr} = S(W_{cl} I_{fused} + b_{cl})$$

$$\mathfrak{L}_{BCE} = -\frac{1}{M}\sum_{i=1}^{M}\left(y_{\text{pr}} \cdot \log(\hat{y}_{\text{pr}}) + (1-y_{\text{pr}}) \cdot \log(1-\hat{y}_{\text{pr}})\right)$$

→ Binary cross-entropy loss

$$\hat{y}_{hr} = W_{hr} I_{fused} + b_{hr}$$

$$\mathfrak{L}_{NLL} = -\frac{1}{M_{E=1}}\sum_{i:E_i=1}\left(\hat{y}_{hr}(i) - \log\left(\sum_{j\in\mathbb{R}(T_j)} e^{\hat{y}_{hr}(j)}\right)\right)$$

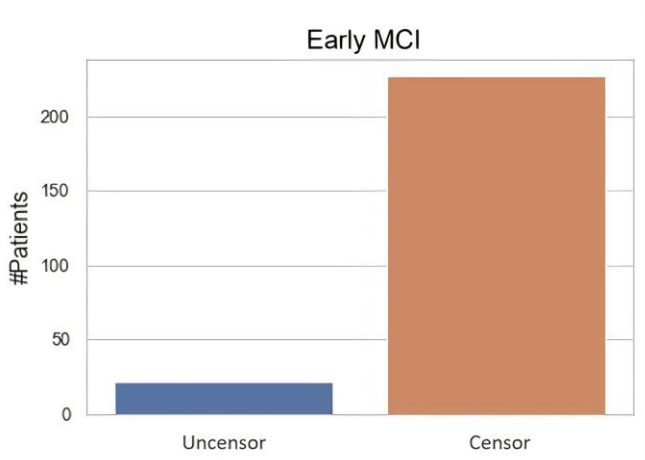
→ Negative log-likelihood loss

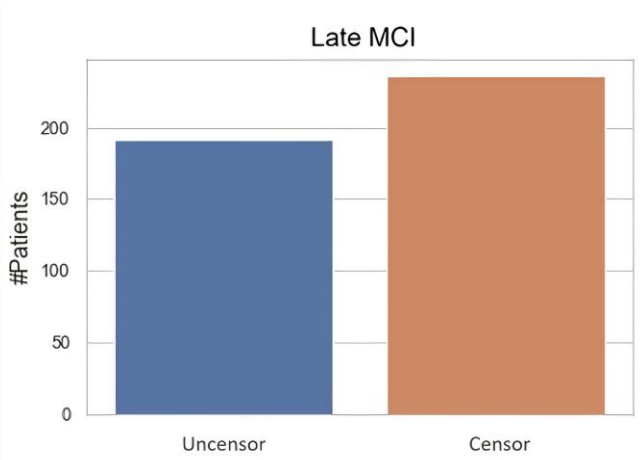
$$\mathfrak{L}_{total} = \mathfrak{L}_{BCE} + \mathfrak{L}_{NLL}$$

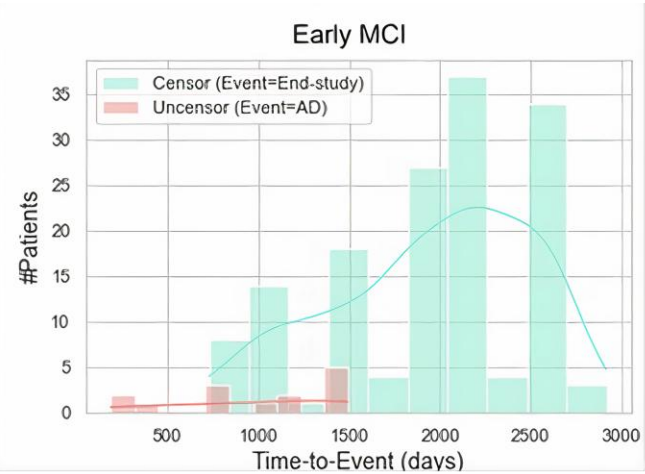
Multimodal MCI-to-AD Prediction

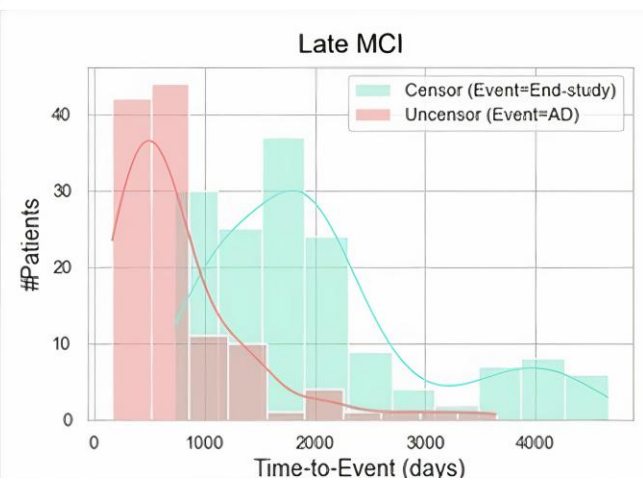
Dataset – ADNI

Variable	eMCI (n=249)	lMCI (n=427)	*p* value
Male, gender, n (%)	141 (56.6%)	262 (61.4%)	0.259*
Age, years, mean±std	71.8 ± 7.3	74.5 ± 7.3	4.1e-6⊥
Education, years, mean±std	15.9 ± 2.7	15.9 ± 3	0.959⊥
CDRSB, n (%)			0.003*
≤ 1	136 (54.6%)	181 (42.4%)	
MMSE, mean±std	28.2 ± 1.6	27.2 ± 1.8	2.2e-13⊥
ADAS13, mean±std	13.0 ± 5.3	18.6 ± 6.7	6.7e-21⊥
RAVLT, mean±std	5.2 ± 2.4	3.5 ± 2.4	2.5e-19⊥
FAQ, mean±std	2.0 ± 2.9	3.7 ± 4.5	0.001⊥
Volumetric biomarker, ml, median (IQR)			
Ventricles, $\times 10^3$	31.2 [19.6, 46.9]	39.1 [27.1, 57.7]	9.0e-6⊣
Hippocampus, $\times 10^3$	7.2 [6.6, 7.8]	6.5 [5.8, 7.2]	4.6e-5⊣
Entorhinal, $\times 10^3$	3.8 [3.3, 4.2]	3.4 [2.8, 3.9]	4.5e-4⊣
Fusiform, $\times 10^3$	18.7[16.8, 20.4]	16.9 [15.0, 18.4]	4.0e-7⊣
Middle Temporal, $\times 10^3$	20.5 [19.1, 22.5]	19.0 [17.1, 21.0]	5.5e-5⊣
Whole Brain, $\times 10^5$	10.6 [9.9, 11.3]	10.0 [9.3, 10.9]	1.3e-8⊣
PET biomarker, median (IQR)			
FDG	1.3 [1.21, 1.35]	1.2 [1.13, 1.3]	2.5e-3⊣
AV45	1.1 [1.01, 1.31]	1.3 [1.07, 1.5]	0.⊣











Multimodal MCI-to-AD Prediction

Time-to-AD conversion

Evaluation:

- CI : concordance index - computes the ability to correctly provide a reliable ranking of the conversion times based on the individual risk scores
- BS : Brier score - evaluates the accuracy of a predicted conversion function at a given time

Approach	Modality	Dataset	Prediction criteria	
			CI↑	BS↓
Polsterl et al.[35]	3D Hippocampus Clinical	397 MCI patients - Censoring rate: unknown	0.803	–
Lu et al.[36]	MRI Genetic	173 MCI patients - Censoring rate: 89%	0.681	0.147
Nakagawa et al.[37]	GM (MRI) Age, MMSE	2, 142 patients (NC, MCI) - Censoring rate: 75% 1, 211 MCI patients - Censoring rate: 58.6%	0.83 0.75	–
Ho et al.[38]	Demographics Biomarkers	1, 334 patients (NC, MCI, AD) - Censoring rate: 74%	0.804	0.153
Ours (SPAN-AED)	Radiomics (MRI) Clinical	249 eMCI patients - Censoring rate: 92% 427 lMCI patients - Censoring rate: 55.3%	**0.846**	**0.132**



Multimodal MCI-to-AD Prediction

EMCI vs LMCI classification

Evaluation:

- Accuracy (Acc) – presents overall effectiveness of a classifier
- AUC - presents how well the probability ranks based on the true classes

Approach	Modality	Dataset (eMCI / lMCI)	Classification criteria Acc↑	AUC↑
Suk et al.[39]	MRI & PET	128 / 76	75.92	0.75
Nozadi et al.[40]	MRI & PET	164 / 189	65.2	–
Jie et al.[41]	rs-fMRI	56 / 43	78.8	0.78
Zhang et al.[42]	rs-fMRI	33 / 29	**83.87**	0.9
Mehmood et al.[18]	GM (MRI)	70 / 70	83.7	–
Cui et al.[43]	MRI	45 / 51	76.13	–
Ours (SPAN-AED)	Radiomics (MRI) Clinical	249 / 427	83.19	**0.91**

Multimodal MCI-to-AD Prediction

Unimodal vs Multimodal

Time-to-AD conversion prediction:

- CI
- BS
- MAE

EMCI vs LMCI classification

- Accuracy (Acc)
- Average Precision (AP)
- Precision (Pre)
- Recall (Rec)
- F_1-score
- AUC

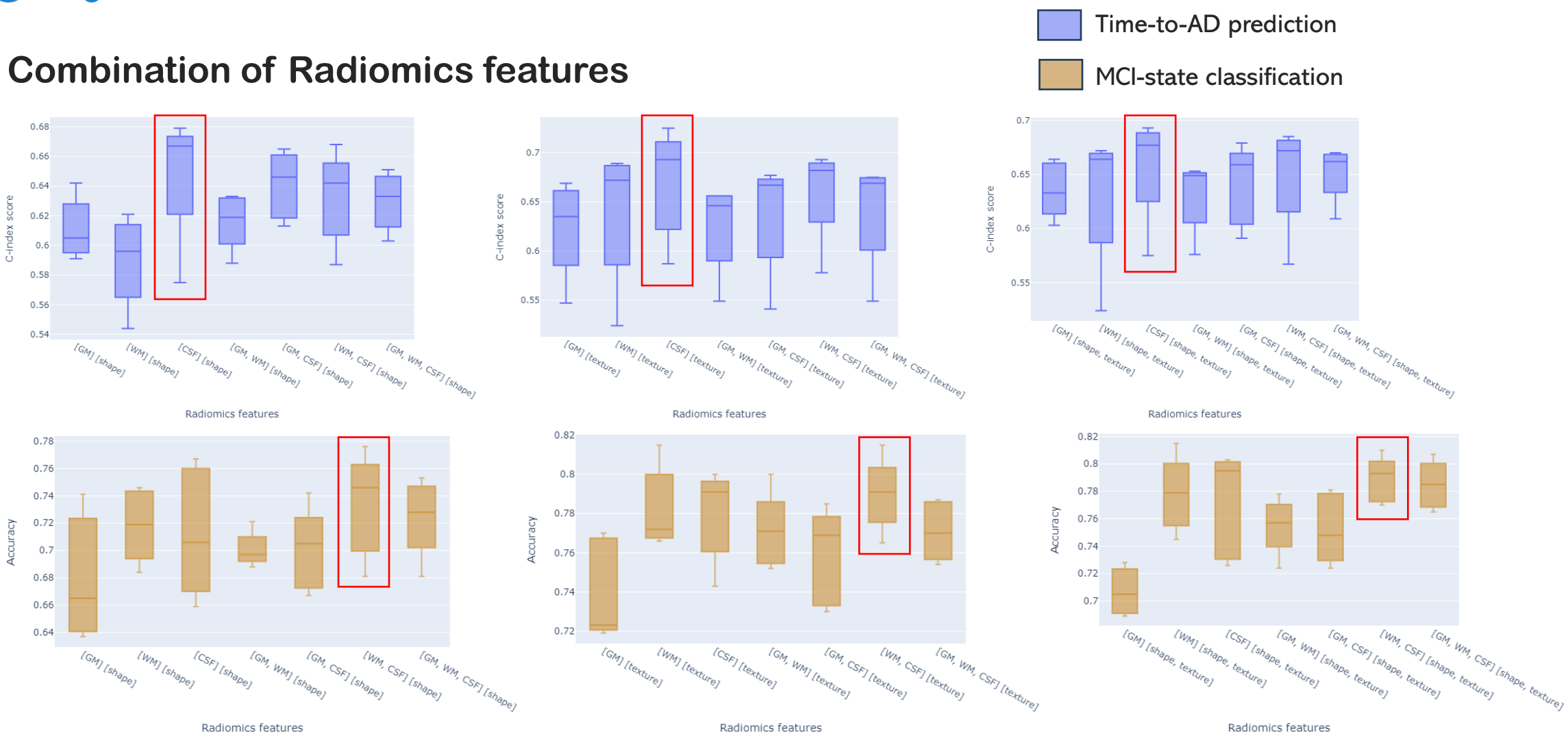
Modality	Approach	Prediction Criteria			Classification criteria					
		CI↑	BS↓	MAE↓	Acc↑	AP↑	Pre↑	Rec↑	F_1 ↑	AUC↑
Clinical	RA	0.8	0.16	510	80.83	91.22	80.67	80.54	80.24	0.88
	SPAN	0.82	0.16	454	81.16	91.53	81.32	81.77	81.53	0.88
Radiomics	RA	0.67	0.2	725	77.21	92.37	76.47	78.23	77.54	84.42
	SPAN	0.67	0.19	669	78.1	92.64	77.81	78.65	78.13	85.46
Multimodal	RA-Concat	0.82	0.16	445	82.35	94.63	80.94	81.86	81.32	0.89
	RA-AED	0.82	0.14	386	83.02	93.68	82.25	**83.44**	**82.51**	0.89
	SPAN-Concat	0.83	0.13	355	82.89	94.14	**83.23**	82.36	82.23	0.9
	Ours(SPAN-AED)	**0.85**	**0.13**	**347**	**83.19**	**94.76**	82.31	82.85	82.47	**0.91**

RA : Residual Attention

Ho, N. H., Jeong, Y. H., Kim, J., Dao, D. P., Pant, S. (2021). "RASurv: Residual Attention-aware Method for Progression-free Survival of Alzheimer's Disease". In: The 5st International Conference on Big data, IoT, and Cloud Computing (BIC'21): Jeju Island, S. Korea, August 16-18, 2021.

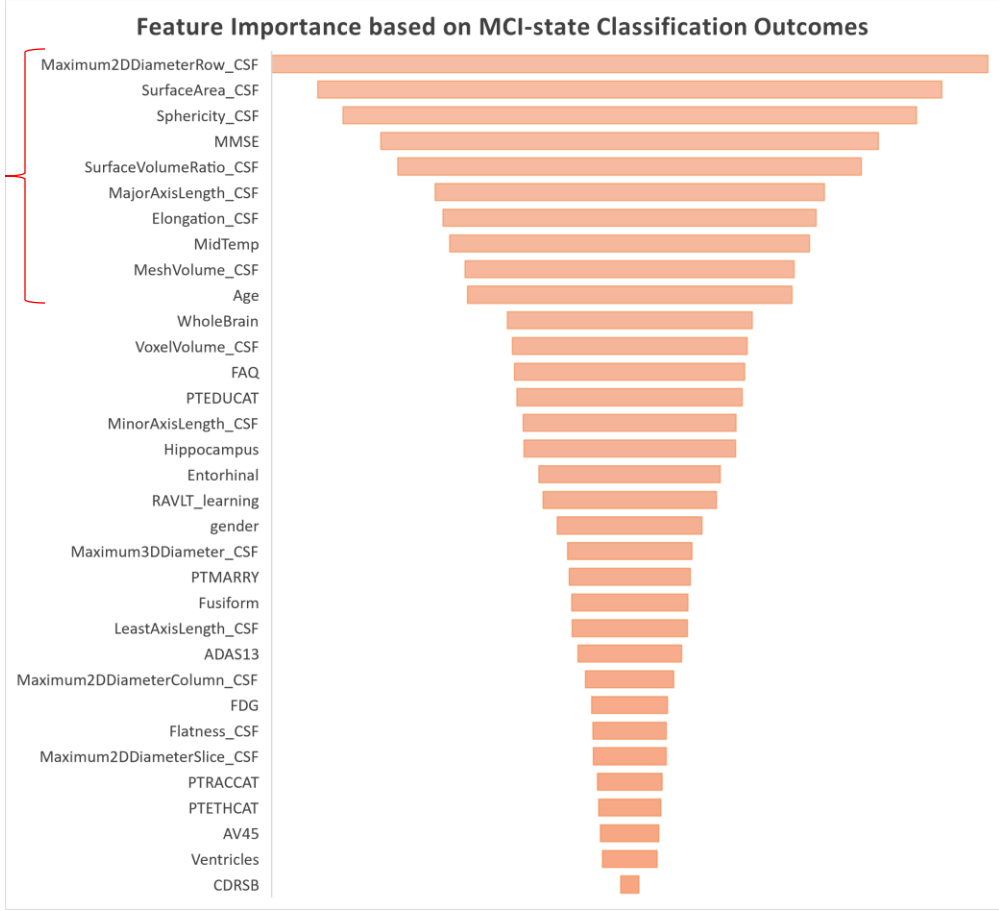
Multimodal MCI-to-AD Prediction

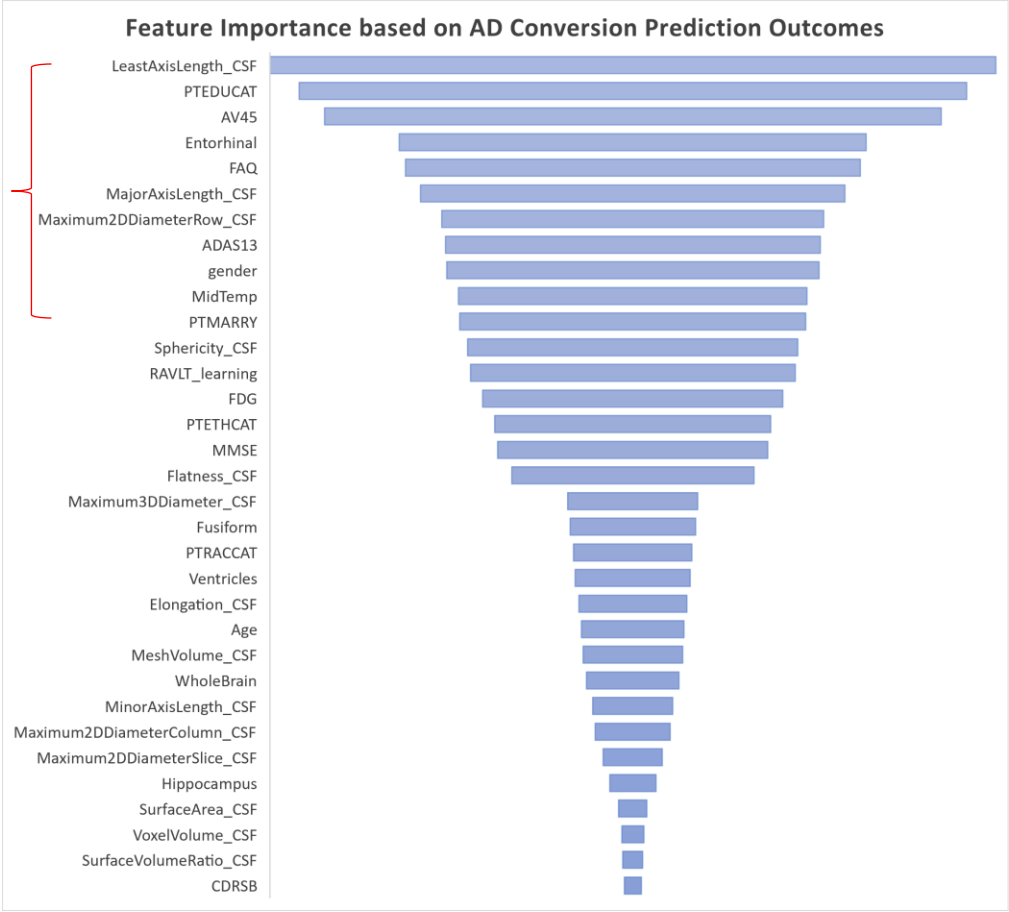
Combination of Radiomics features



Multimodal MCI-to-AD Prediction

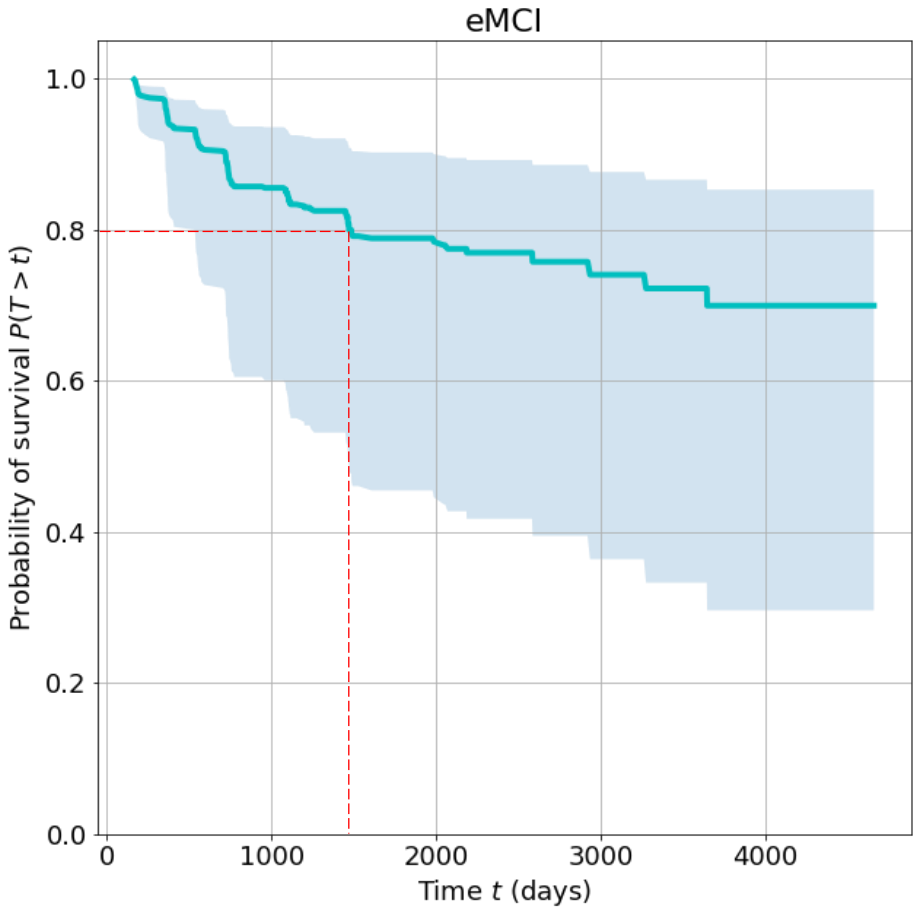
Feature Importance

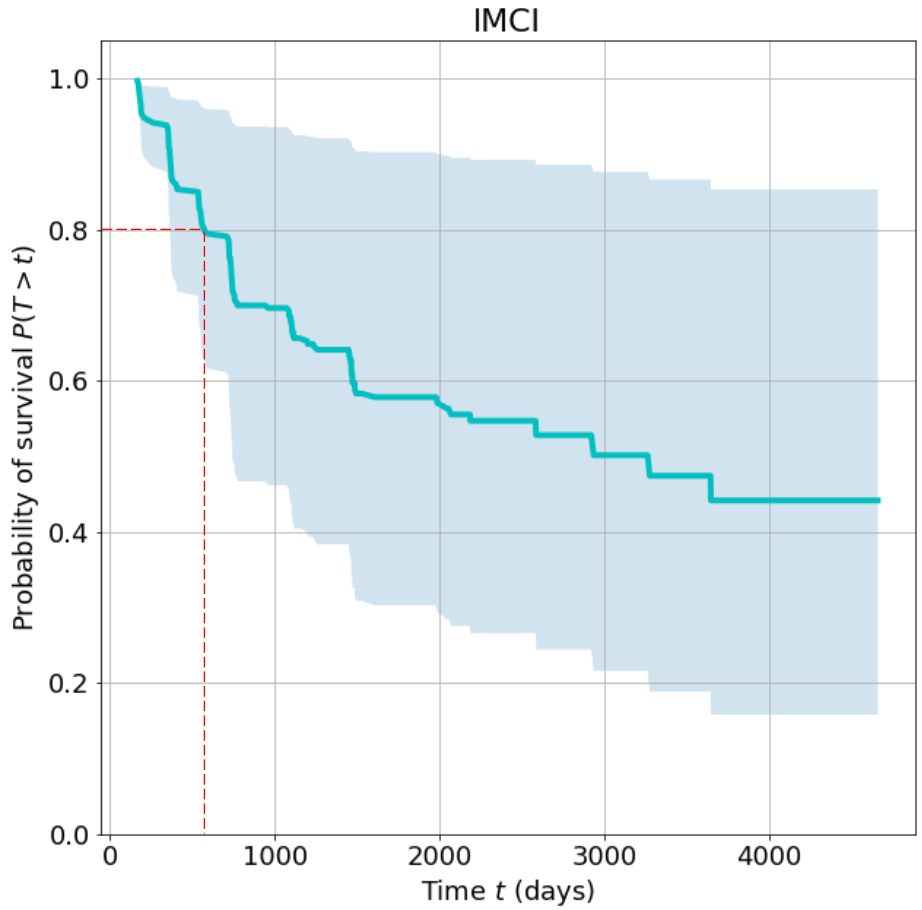




Multimodal MCI-to-AD Prediction

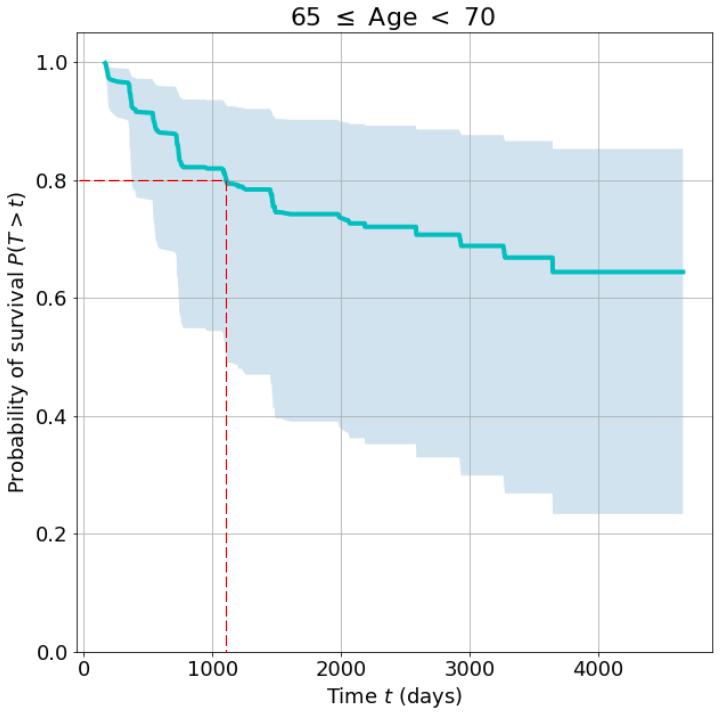
Conversion time prediction – patient status

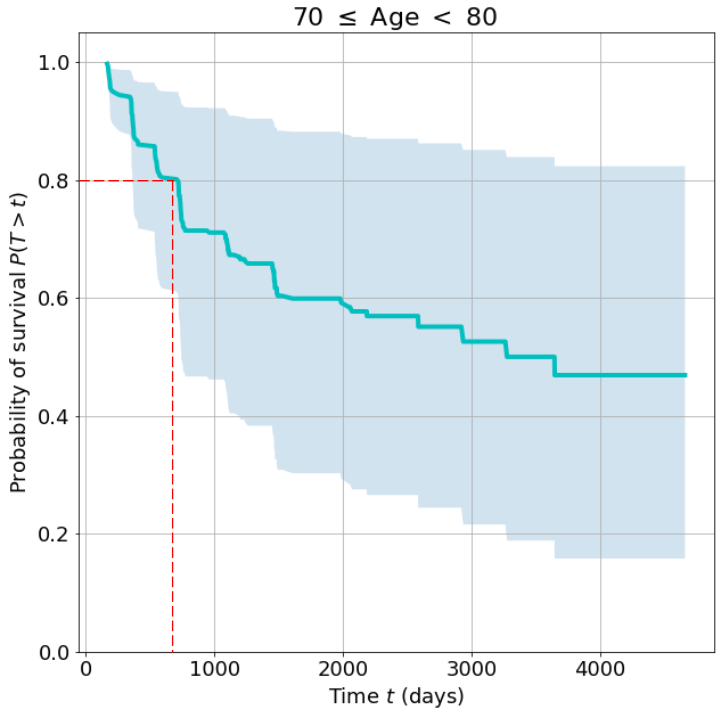


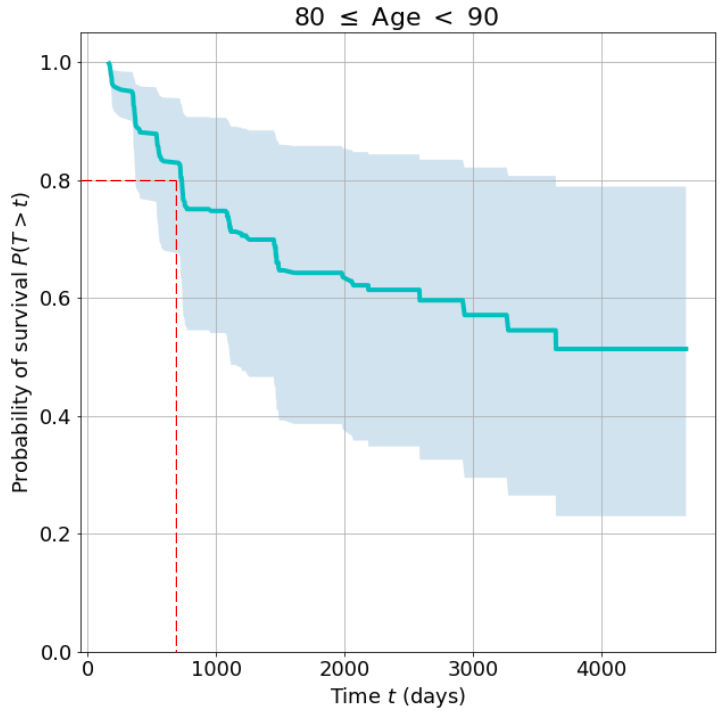


Multimodal MCI-to-AD Prediction

Conversion time prediction - Age

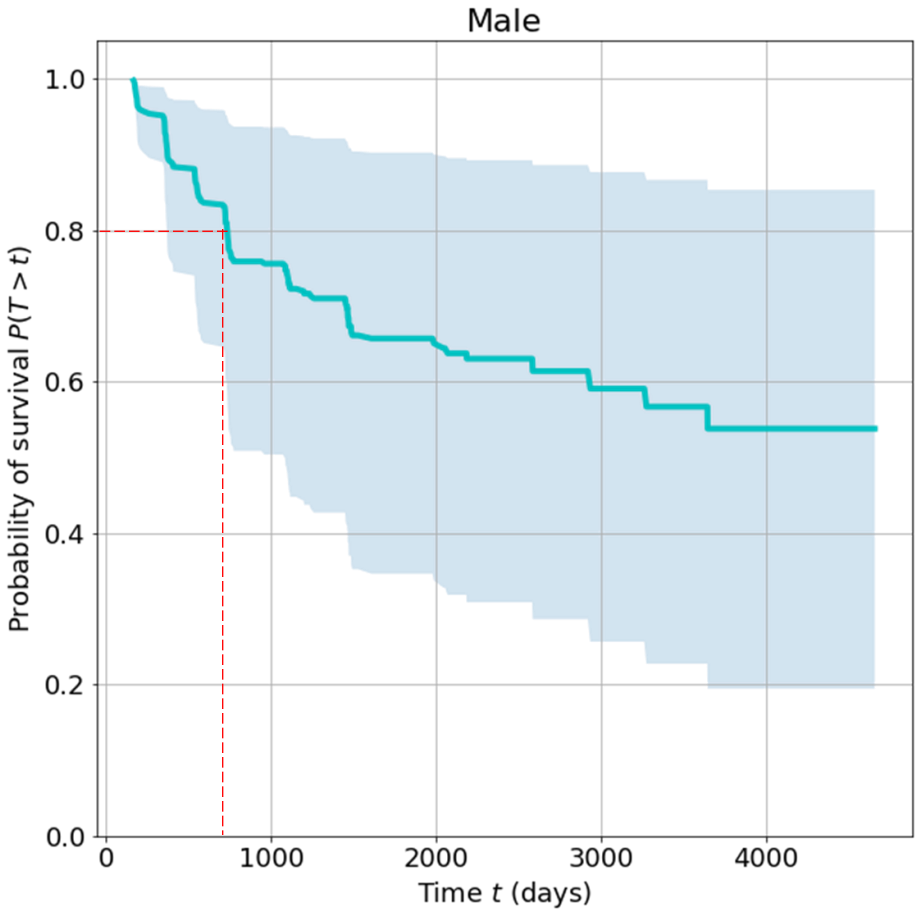


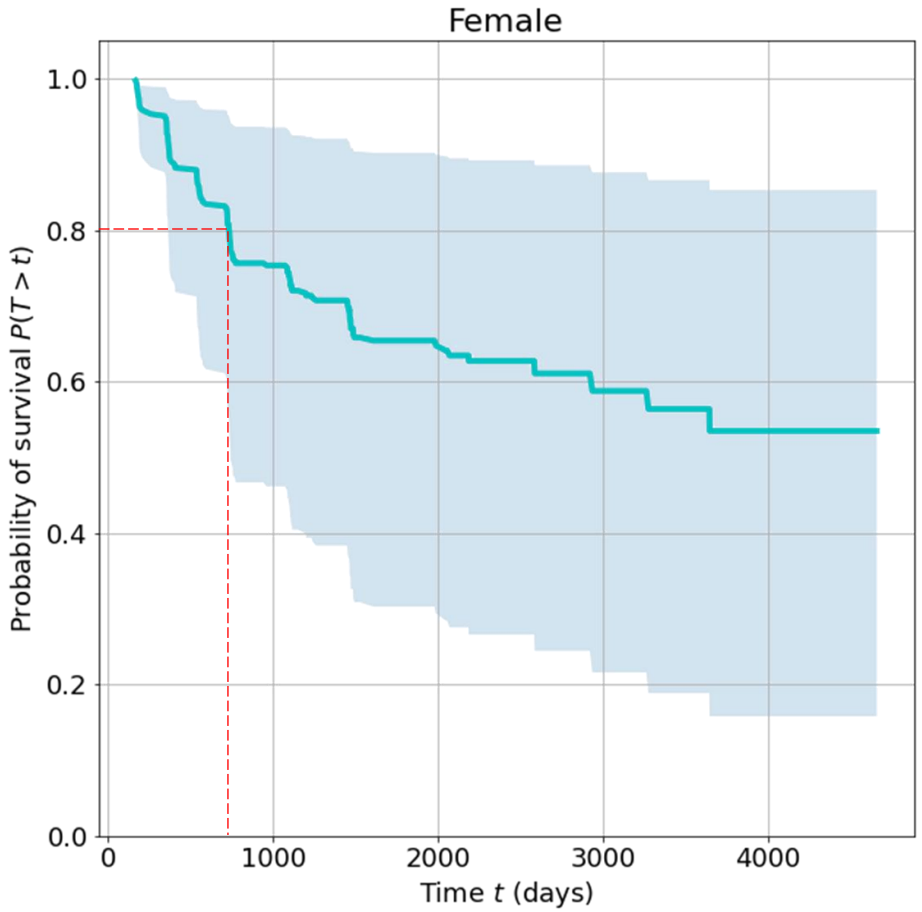




Multimodal MCI-to-AD Prediction

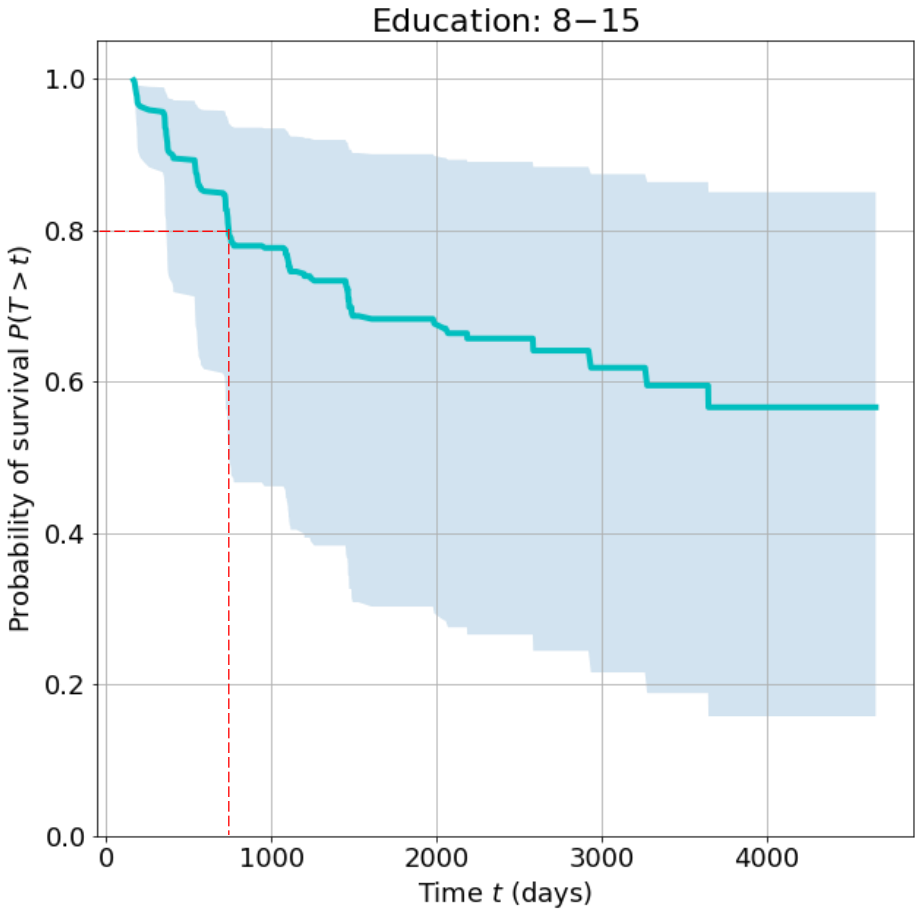
Conversion time prediction - Gender

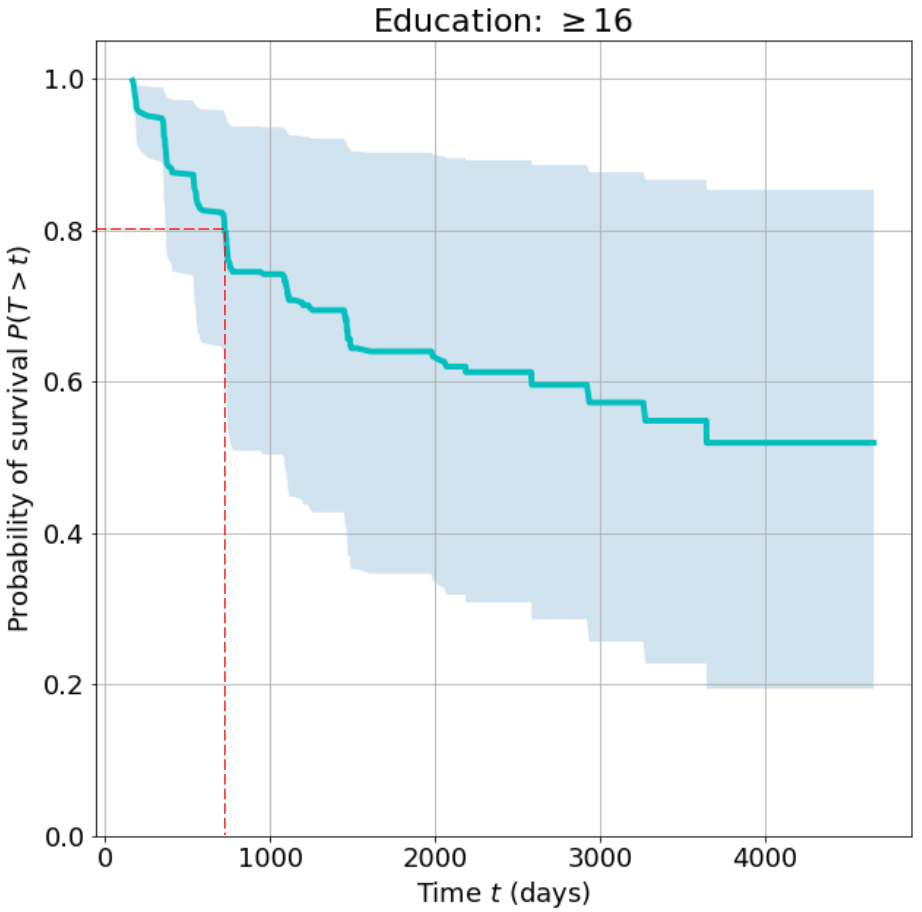




Multimodal MCI-to-AD Prediction

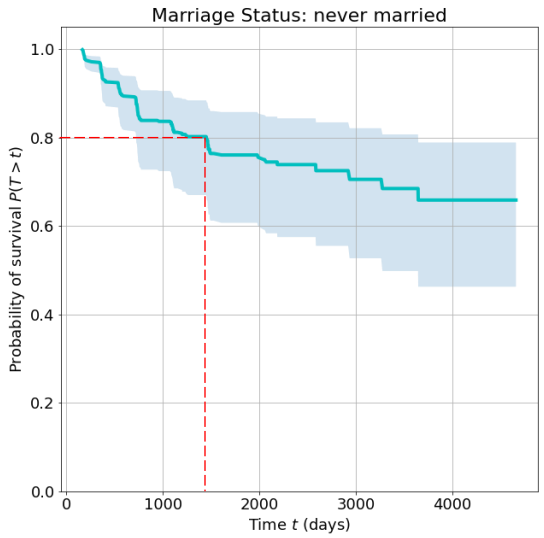
Conversion time prediction - Education

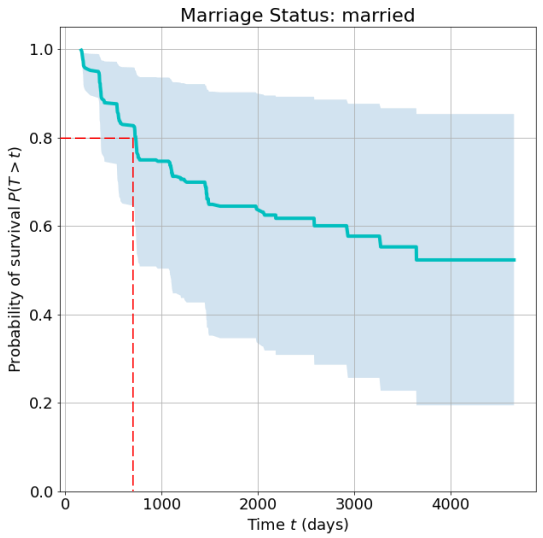


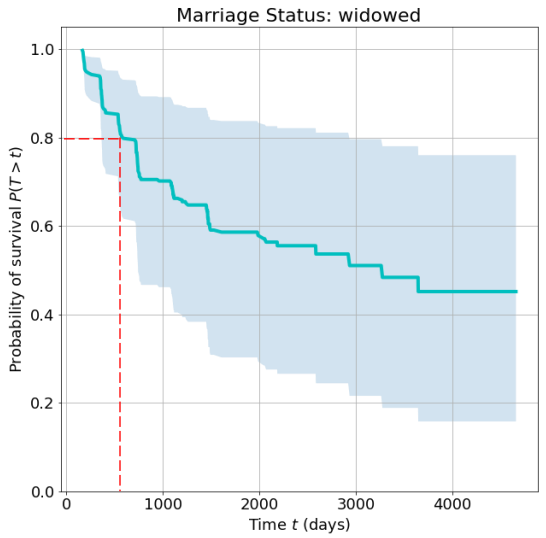


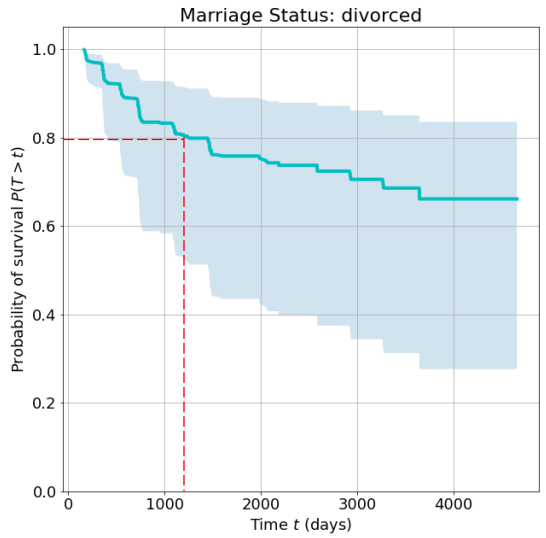
Multimodal MCI-to-AD Prediction

Conversion time prediction – Marriage status



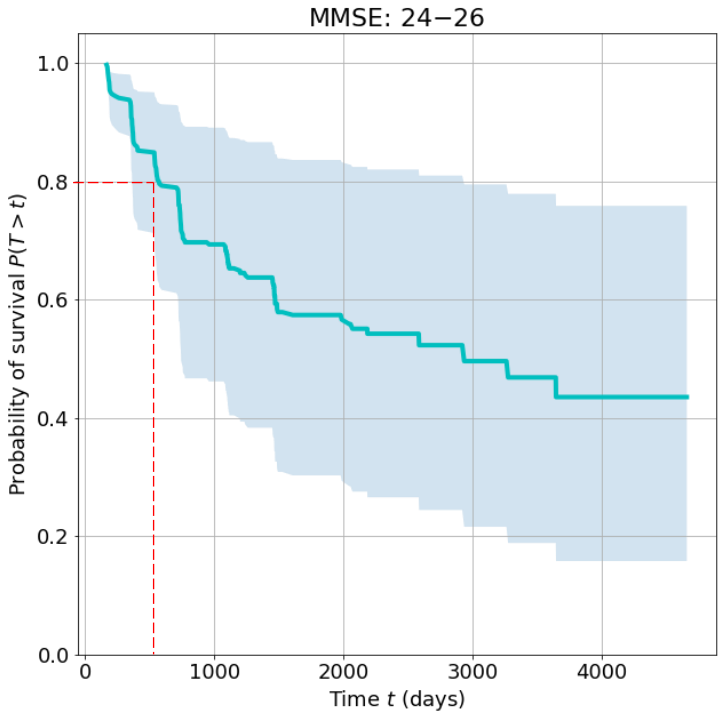


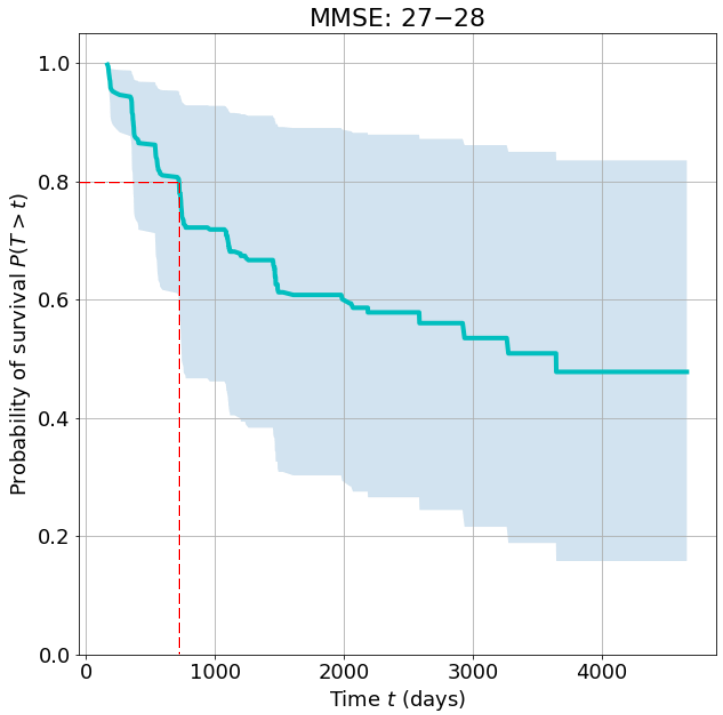


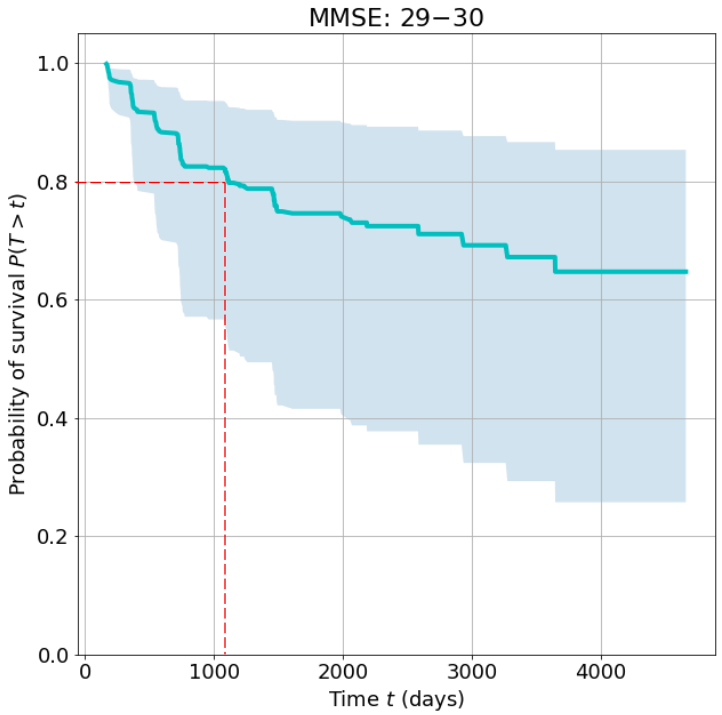


Multimodal MCI-to-AD Prediction

Conversion time prediction – MMSE



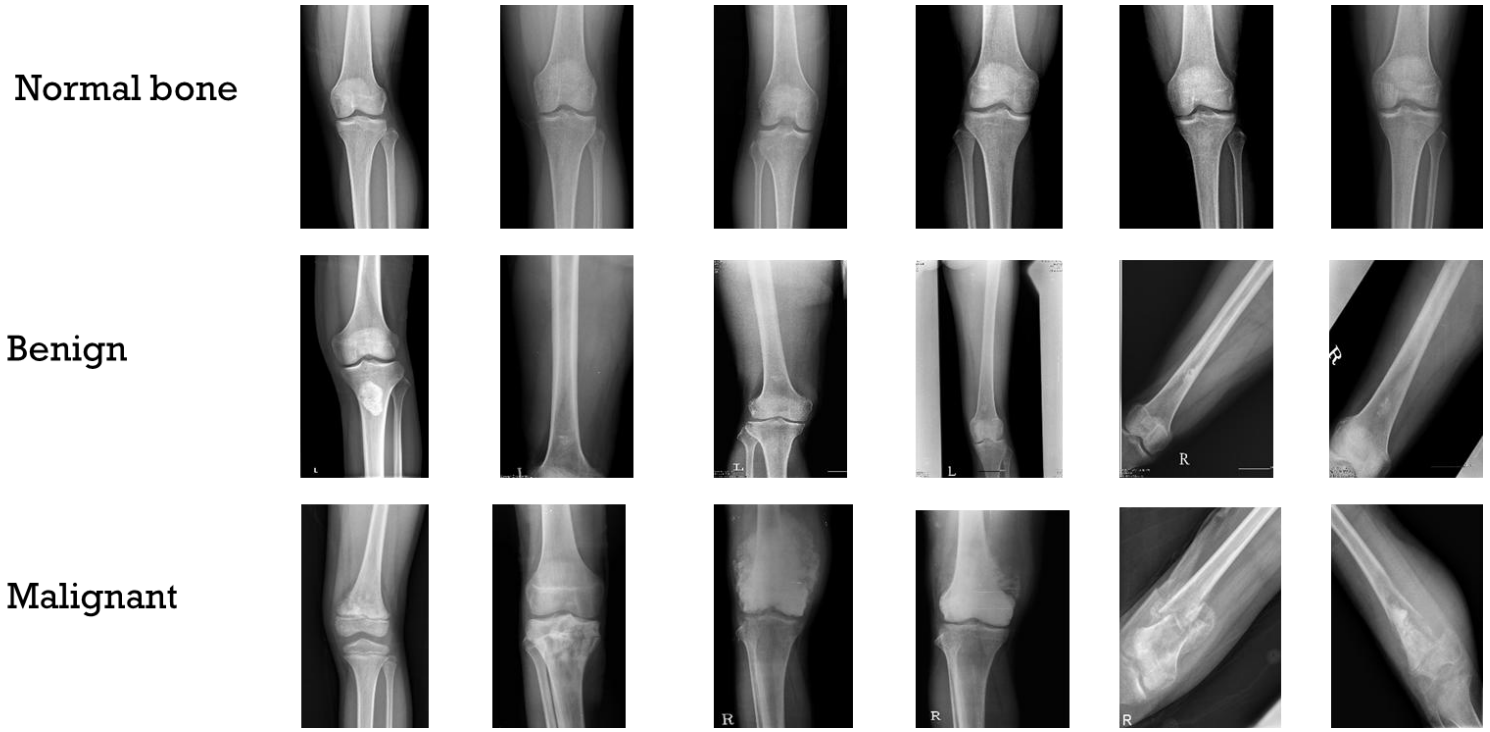






Tumor Detection

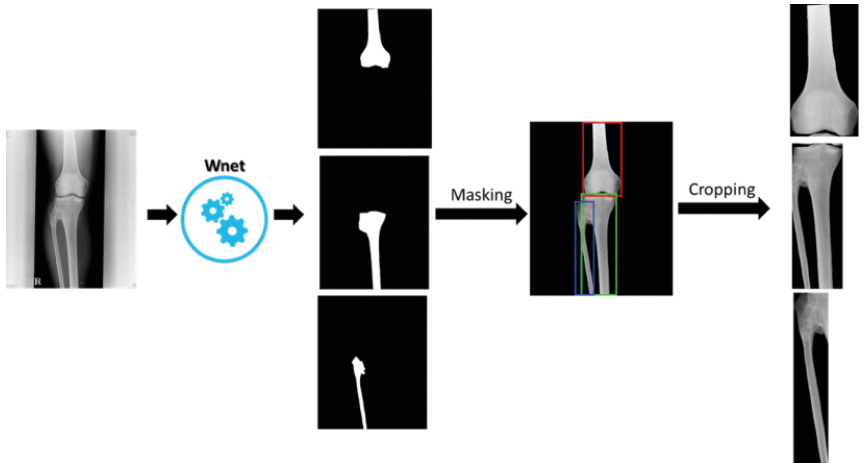
Knee-bone tumor prediction

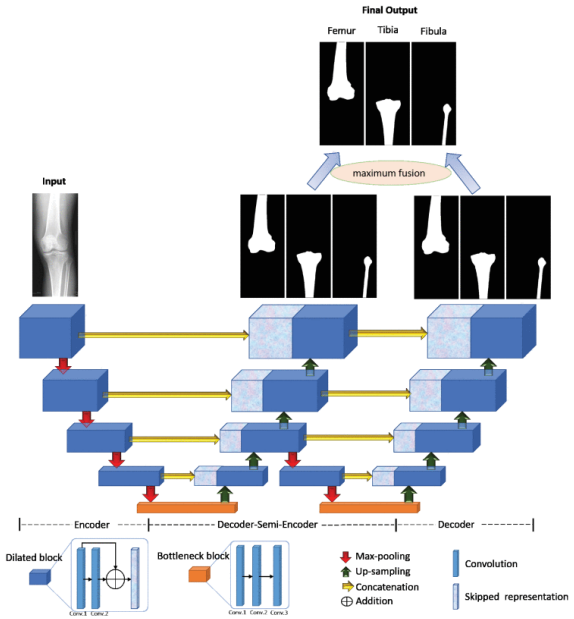


- Identify knee-bone tumor from X-ray scans
- Automatically segment knee regions to determine tumor types: benign and malignant

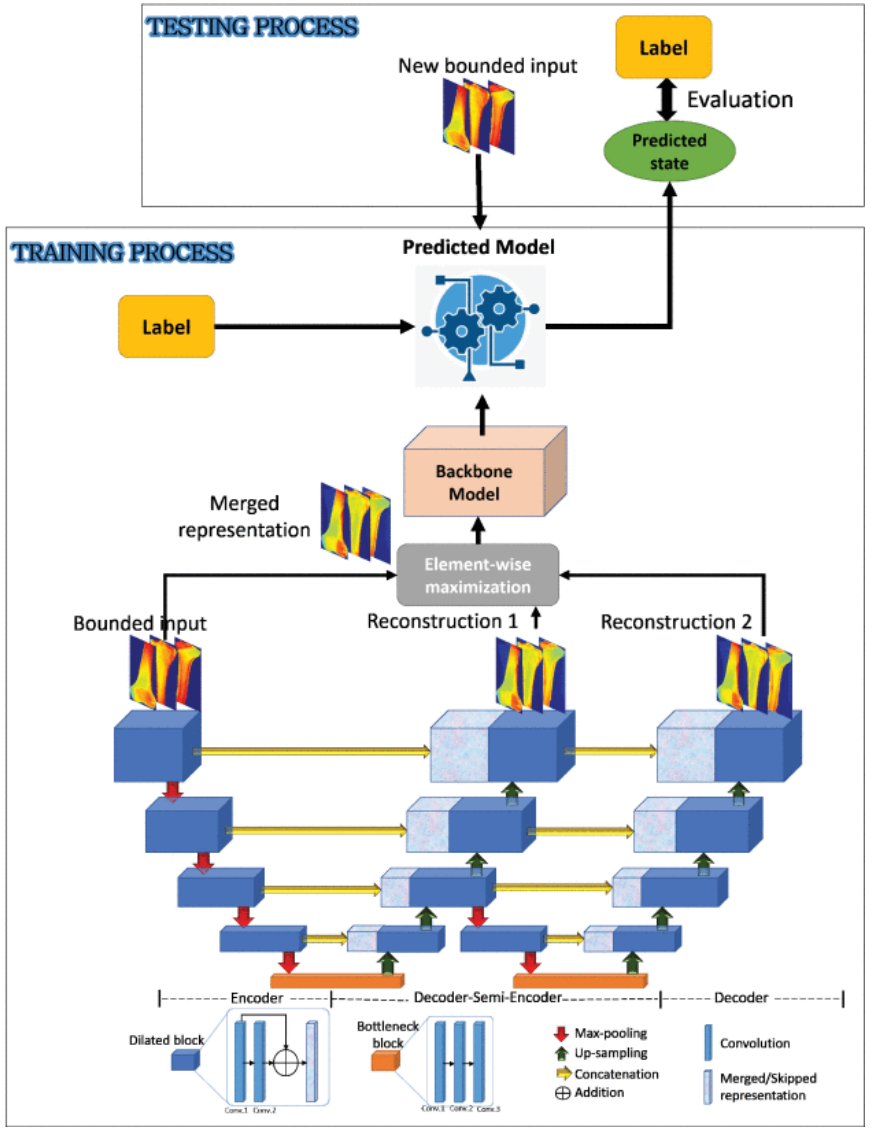
Ho, N.H., Yang, H.J., Kim, S.H., Jung, S.T. and Joo, S.D., 2019. Regenerative semi-supervised bidirectional w-network-based knee bone tumor classification on radiographs guided by three-region bone segmentation. IEEE Access, 7, pp.154277-154289.

Knee-bone tumor prediction





Knee-bone segmentation

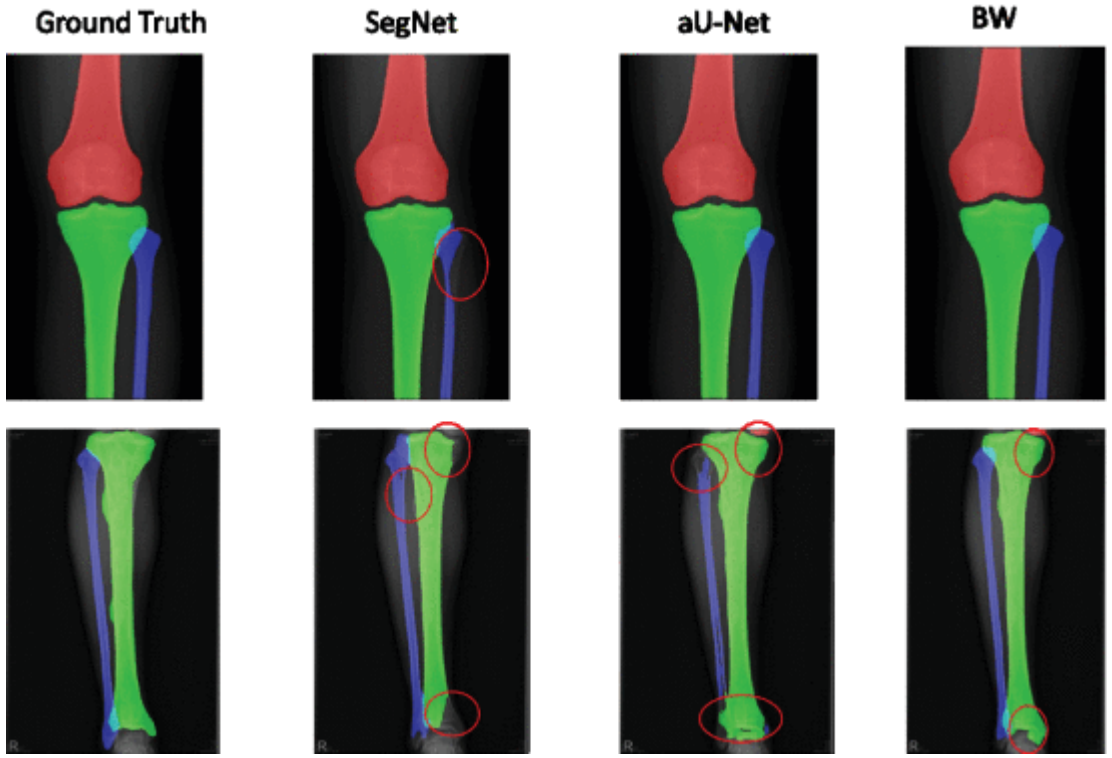


Knee-bone tumor classification

Knee-bone tumor prediction

Performance: Knee-bone segmentation

Model	*Mean Dice Score*	*Sensitivity*	*Specificity*
SegNet	94.31 ± 0.78	95.08 ± 0.92	98.97 ± 0.42
aU-Net	96.83 ± 1.12	96.75 ± 1.15	99.24 ± 1.09
BW (proposed method)	$\mathbf{98.06 \pm 0.08}$	$\mathbf{97.69 \pm 0.15}$	$\mathbf{99.61 \pm 0.03}$



Knee-bone tumor prediction

Performance: Knee-bone tumor classification

Single-step strategy

Model	*Accuracy*	*Precision*	*Recall*	F_β
VGG16-B	**80.54 ± 3.46**	**64.57 ± 5.25**	**71.15 ± 7.48**	**65.9 ± 7.24**
ResNet50-B	75.62 ± 4.52	62.33 ± 4.1	67.84 ± 4.89	63.78 ± 4.64
InceptionV3-B	74.31 ± 4.66	62.18 ± 4.35	67.33 ± 4.22	64.25 ± 4.72
VGG16-R	79.13 ± 2.54	58.46 ± 2.13	61.27 ± 5.56	59.78 ± 6.2
ResNet50-R	72.53 ± 4.66	52.78 ± 4.23	58.18 ± 6.86	52.99 ± 6.72
InceptionV3-R	70.29 ± 5.13	52.34 ± 4.55	57.33 ± 6.74	54.87 ± 6.89

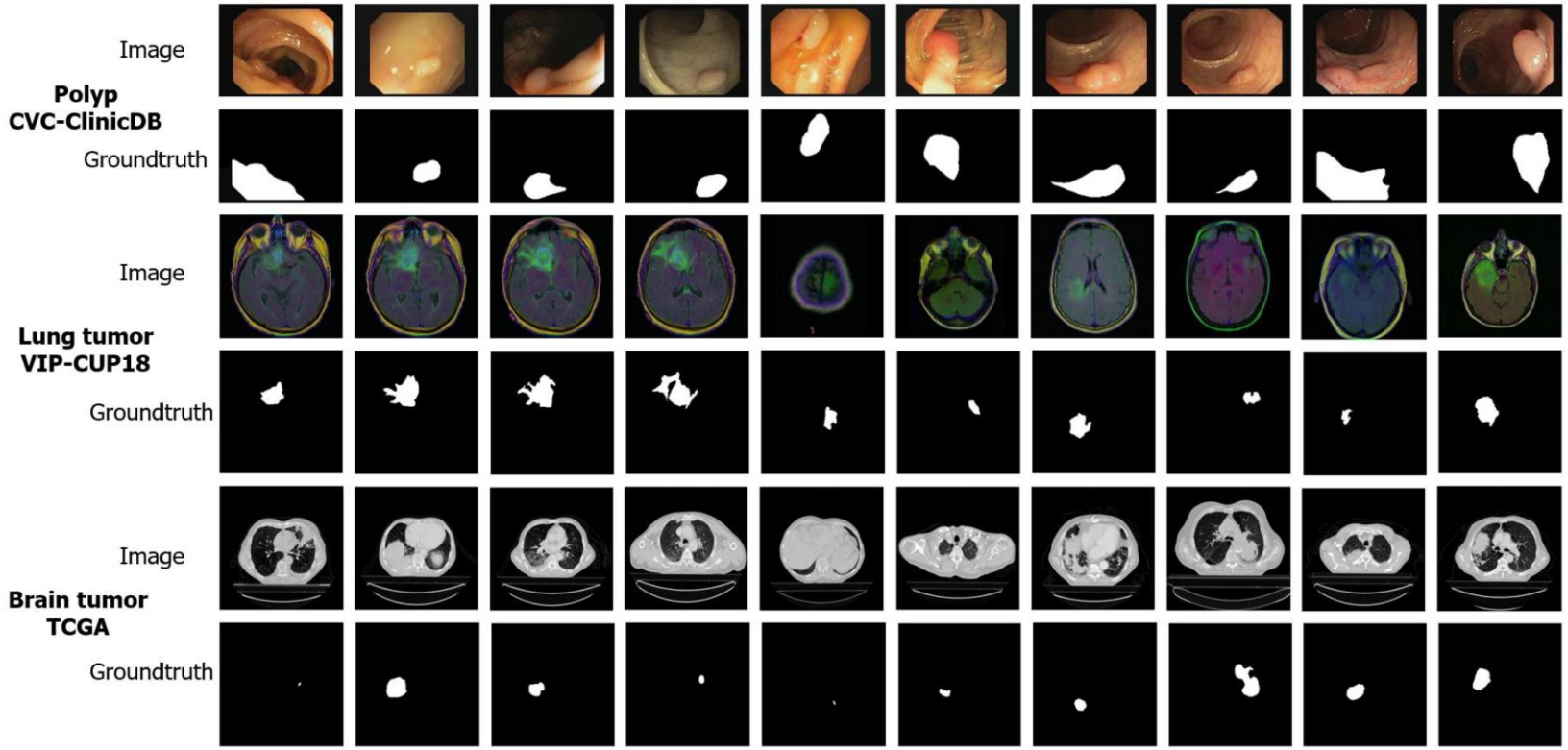
Single-step strategy + RSS-BW

Model	*Accuracy*	*Precision*	*Recall*	F_β
RSS-BW+VGG16-B	**85.23 ± 3.91**	**82.23 ± 3.22**	**82.15 ± 3.31**	**82.21 ± 3.25**
RSS-BW+ResNet50-B	82.2 ± 3.98	80.15 ± 3.35	81.17 ± 3.62	80.33 ± 3.23
RSS-BW+InceptionV3-B	81.65 ± 4.03	80.12 ± 4.17	79.38 ± 3.45	79.67 ± 3.55
RSS-BW+VGG16-R	83.27 ± 3.65	81.05 ± 2.38	81.41 ± 3.75	81.32 ± 3.13
RSS-BW+ResNet50-R	80.61 ± 4.77	79.52 ± 3.45	80.44 ± 3.21	80.11 ± 3.51
RSS-BW+InceptionV3-R	79.82 ± 4.84	78.49 ± 3.68	80.02 ± 3.46	79.63 ± 3.44

Double-step strategy + RSS-BW

Model		*Accuracy*	*Precision*	*Recall*	F_β
RSS-BW +VGG16-B	First state	98.79 ± 0.22	98.58 ± 0.39	98.56 ± 0.4	98.69 ± 0.27
	Second state	84.77 ± 1.35	83.6 ± 5.42	83.62 ± 2.15	83.63 ± 2.37
	Final result	**86.93 ± 2.47**	**85.24 ± 3.55**	**85.56 ± 2.84**	**85.29 ± 2.15**
RSS-BW +ResNet50-B	First state	93.64 ± 0.73	93.88 ± 0.57	93.41 ± 0.59	93.47 ± 0.43
	Second state	78.43 ± 5.66	78.23 ± 3.46	77.94 ± 4.26	78.12 ± 5.48
	Final result	82.31 ± 3.64	81.46 ± 3.25	81.24 ± 3.86	81.79 ± 3.16
RSS-BW +InceptionV3-B	First state	93.17 ± 0.84	93.25 ± 0.66	93.48 ± 0.54	93.36 ± 0.62
	Second state	77.84 ± 5.53	77.15 ± 3.91	78.52 ± 3.66	77.69 ± 4.31
	Final result	81.58 ± 3.25	80.62 ± 3.41	81.09 ± 3.67	80.89 ± 3.48

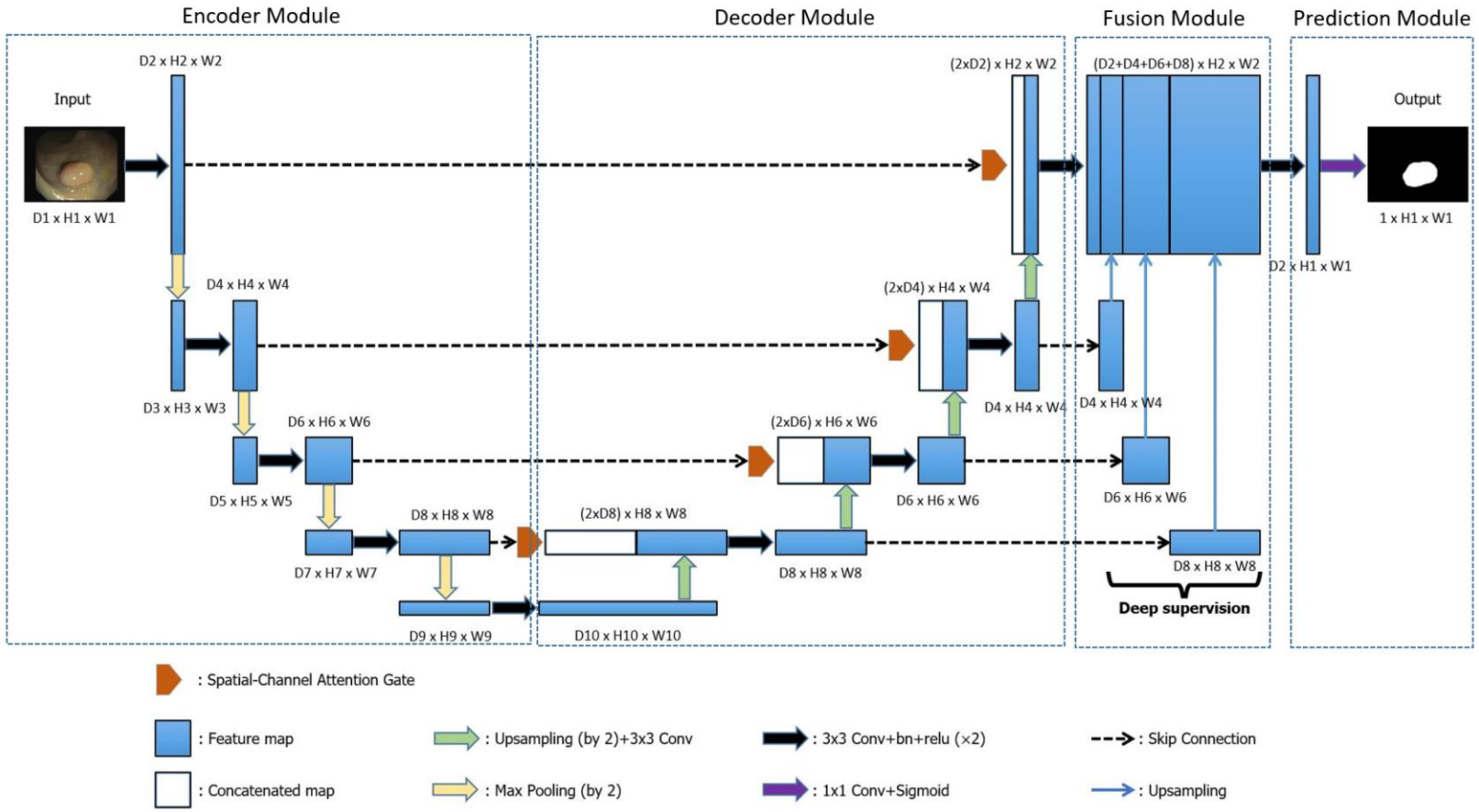
Abnormal tissue segmentation



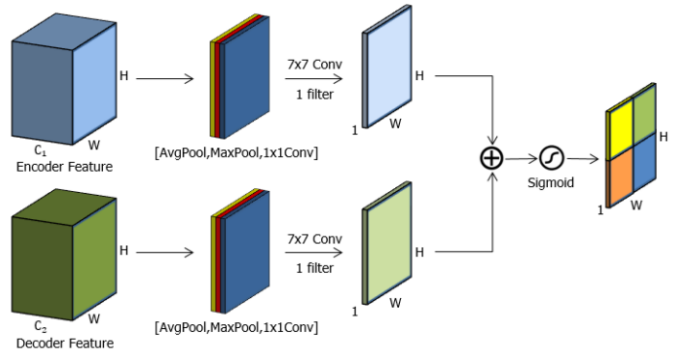
- Segment abnormal tissue at image-level
- Enhance Unet with Spatial-Channel attention

Khanh, T.L.B., Dao, D.P., Ho, N.H., Yang, H.J., Baek, E.T., Lee, G., Kim, S.H. and Yoo, S.B., 2020. Enhancing U-Net with spatial-channel attention gate for abnormal tissue segmentation in medical imaging. Applied Sciences, 10(17), p.5729.

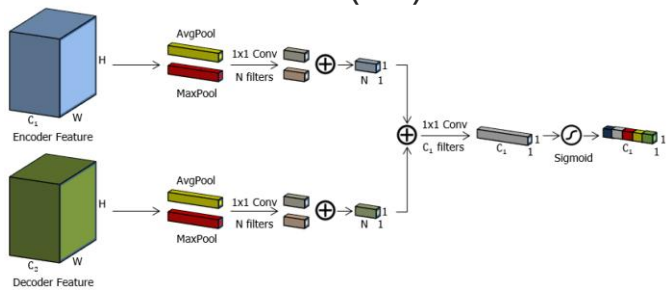
Abnormal tissue segmentation



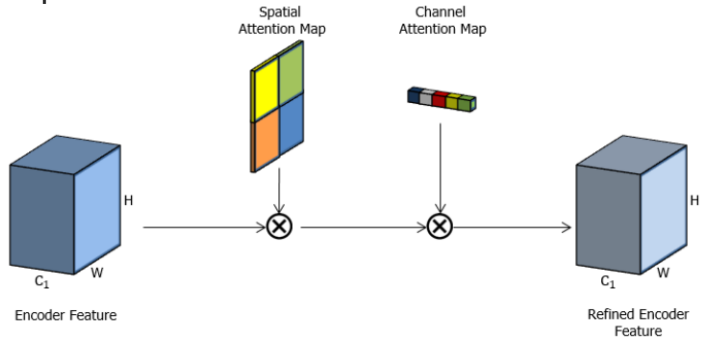
Spatial Attention Gate (sAG)



Channel Attention Gate (cAG)



Spatial-Channel Attention

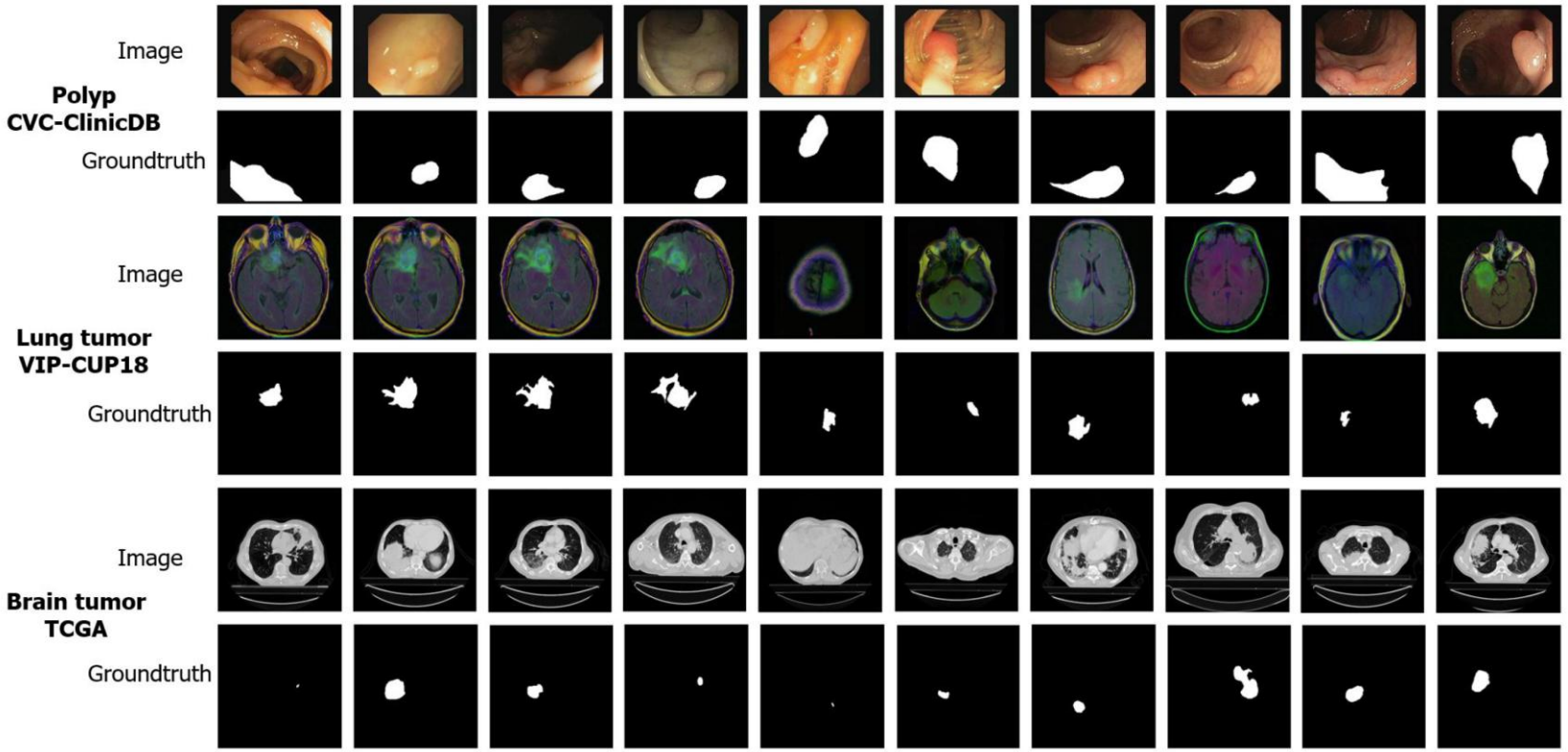


Abnormal tissue segmentation

Datasets

Table 1. Overview of the datasets.

Dataset	Application	No. of Images	Input Resolution	Modality
CVC-ClinicDB [29]	Polyp	612	256 × 192	Endoscopy
VIP-CUP18 [30]	Lung tumor	5204	256 × 256	CT
TCGA [31]	Brain tumor	1373	256 × 256	MRI



Abnormal tissue segmentation

Performance:

Comparison with other methods

Model	Deep Supervision	Dataset	Dice Score (%)	Precision (%)	Recall (%)
U-Net [11]	×	CVC-ClinicDB	65.93 ± 6.34	61.49 ± 7.30	70.00 ± 6.62
		VIP-CUP18	52.47 ± 3.83	48.14 ± 6.45	54.44 ± 3.40
		TCGA	83.52 ± 1.61	77.79 ± 2.90	83.44 ± 2.30
Attention U-Net [17,18]	×	CVC-ClinicDB	67.57 ± 6.47	64.03 ± 7.13	71.68 ± 5.96
		VIP-CUP18	53.15 ± 3.21	47.52 ± 3.24	54.75 ± 4.03
		TCGA	83.88 ± 1.72	78.42 ± 2.91	82.27 ± 2.61
U-Net++ [15,16]	×	CVC-ClinicDB	68.89 ± 6.87	66.18 ± 7.40	71.61 ± 5.68
		VIP-CUP18	54.66 ± 3.77	49.89 ± 5.47	55.87 ± 2.23
		TCGA	84.54 ± 1.62	79.47 ± 2.45	82.50 ± 2.42
U-Net+scAG (Proposed)	×	CVC-ClinicDB	71.72 ± 6.81	69.81 ± 8.97	74.21 ± 4.56
		VIP-CUP18	55.89 ± 3.97	51.41 ± 6.81	$\mathbf{58.24 \pm 1.82}$
		TCGA	85.18 ± 1.31	81.74 ± 1.89	83.84 ± 3.33
U-Net+scAG (Proposed)		CVC-ClinicDB	$\mathbf{73.31 \pm 5.85}$	$\mathbf{72.43 \pm 7.14}$	$\mathbf{76.82 \pm 2.94}$
		VIP-CUP18	$\mathbf{56.26 \pm 3.51}$	$\mathbf{51.79 \pm 4.42}$	57.11 ± 3.54
		TCGA	$\mathbf{85.83 \pm 1.41}$	$\mathbf{83.74 \pm 1.81}$	$\mathbf{83.86 \pm 2.46}$

Latency of inference consumption

Model	Deep Supervision	No. of Parameters	Inference Time(ms/img)		
			CVC-ClinicDB	VIP-CUP18	TCGA
U-Net [11]	×	8637×10^6	15	15	14
Attention U-Net [17,18]	×	8726×10^6	22	21	21
U-Net++ [15,16]	×	$10,198 \times 10^6$	28	26	26
U-Net+scAG (Proposed)	×	8656×10^6	33	32	32
U-Net+scAG (Proposed)		8804×10^6	34	33	34

Abnormal tissue segmentation

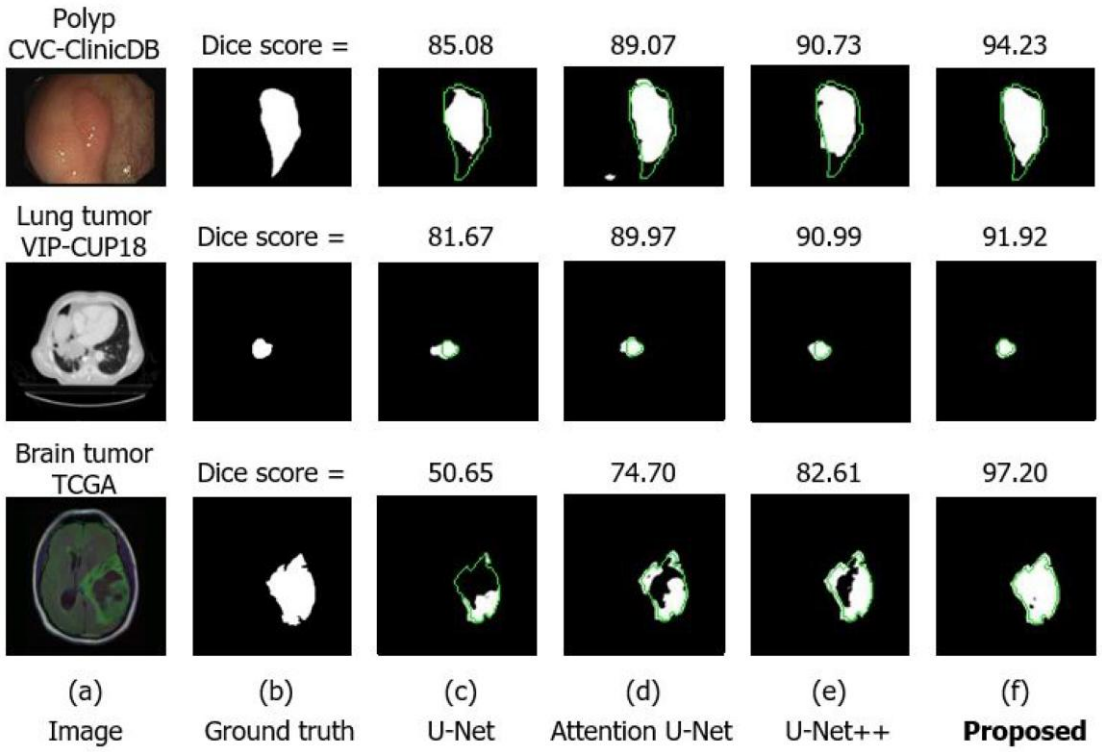
Performance:

Comparison with different channel ratio

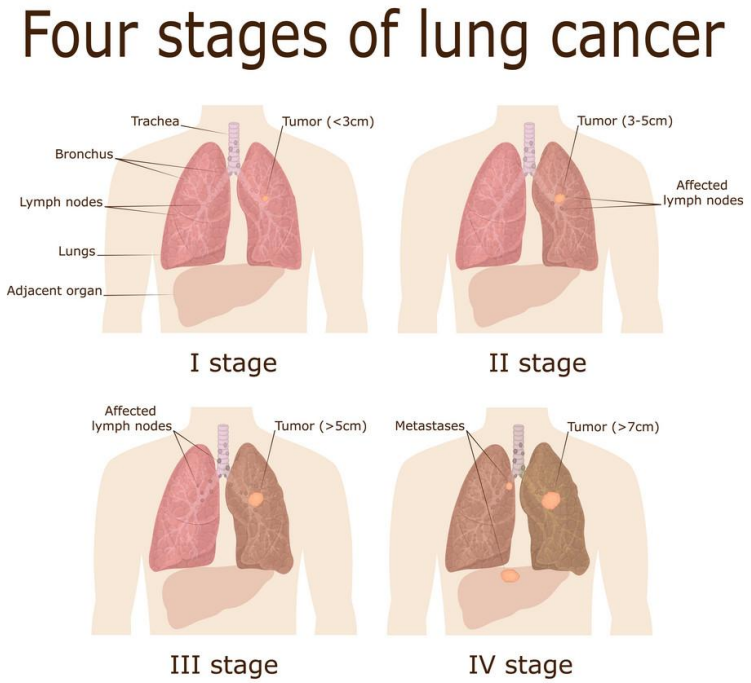
Model	Dice Score (%)	Precistion (%)	Recall (%)
U-Net + spatial + channel (ratio = 16)	**71.72 ± 6.81**	69.81 ± 8.97	**74.21 ± 4.56**
U-Net + spatial + channel (ratio = 8)	70.55 ± 4.98	**70.44 ± 6.29**	73.04 ± 5.52
U-Net + spatial + channel (ratio = 2)	70.76 ± 5.98	70.05 ± 9.76	73.97 ± 3.80

Comparison with different spatial parameters

Model	Dice Score (%)	Precistion (%)	Recall (%)
U-Net + spatial (avg-max) + channel	70.18 ± 4.63	**71.52 ± 8.66**	72.04 ± 3.13
U-Net + spatial (1 × 1 conv) + channel	70.15 ± 5.49	67.62 ± 8.21	73.94 ± 4.84
U-Net + spatial (avg-max-conv) + channel	**71.72 ± 6.81**	69.81 ± 8.97	**74.21 ± 4.56**
U-Net + spatial (k = 7) + channel	**71.72 ± 6.81**	69.81 ± 8.97	**74.21 ± 4.56**
U-Net + spatial (k = 5) + channel	70.47 ± 5.12	70.05 ± 7.32	73.35 ± 5.14
U-Net + spatial (k = 3) + channel	70.94 ± 6.20	**71.06 ± 10.00**	73.31 ± 3.94



Non-small cell lung cancer prediction



- Abnormal Tissue Segmentation in non-small cell lung cancer patient
- Survival analysis using segmented tissue region and clinical data

Dao, Duy-Phuong, Hyung-Jeong Yang, Ngoc-Huynh Ho, Sudarshan Pant, Soo-Hyung Kim, Guee-Sang Lee, In-Jae Oh, and Sae-Ryung Kang. "Survival Analysis based on Lung Tumor Segmentation using Global Context-aware Transformer in Multimodality." In 2022 26th International Conference on Pattern Recognition (ICPR), pp. 5162-5169. IEEE, 2022.

Non-small cell lung cancer prediction

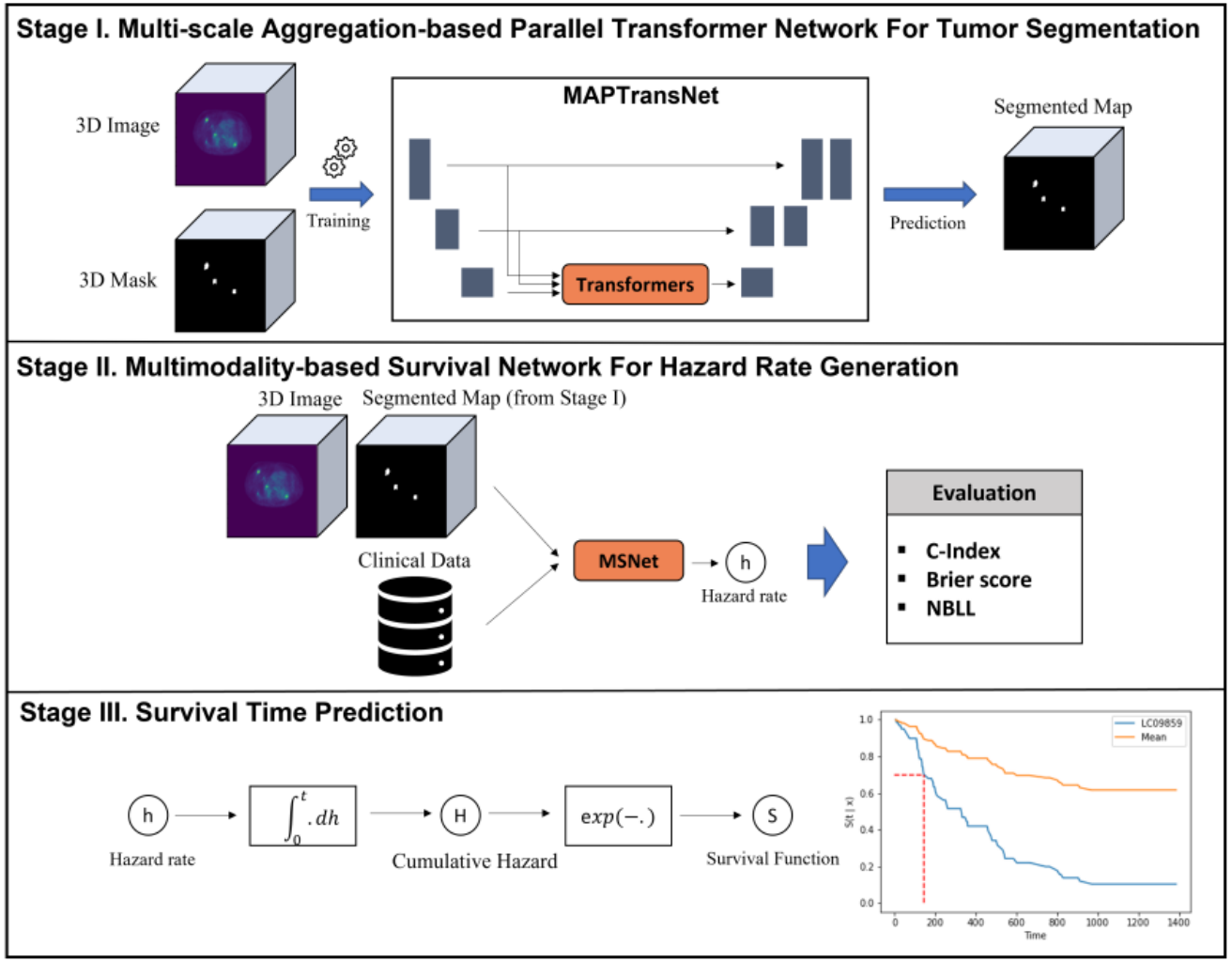


Fig. 1. The overall network architecture. Our proposed method consists of three stages, as illustrated above.

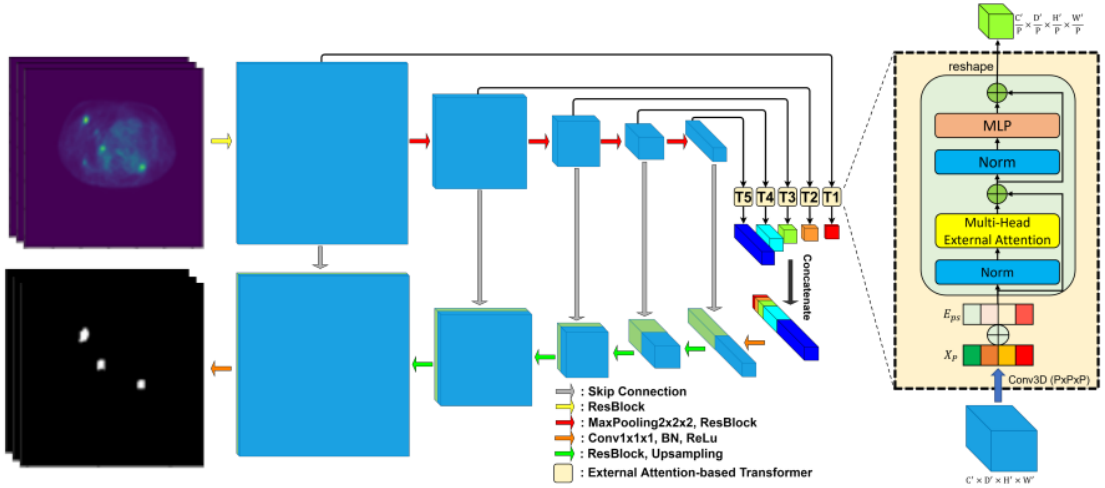


Fig. 2. The architecture of MAPTransNet model.

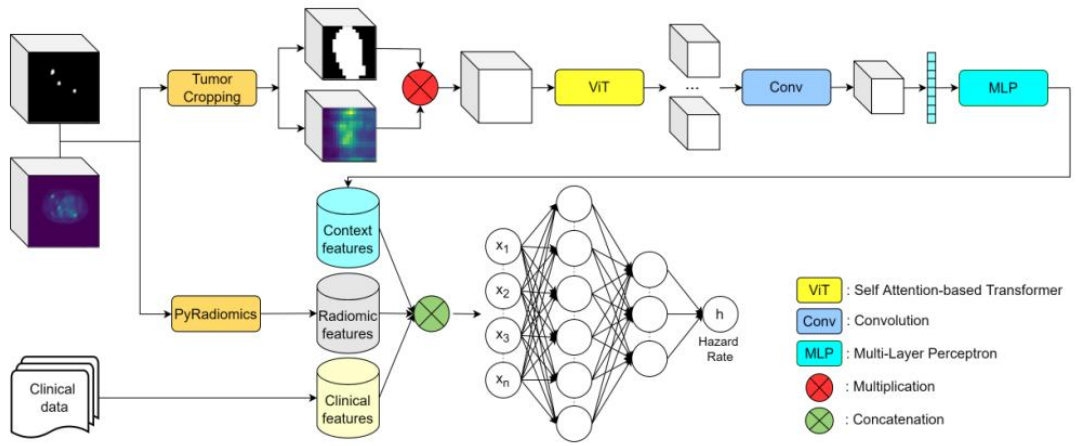


Fig. 3. The architecture of MSNet model.

Non-small cell lung cancer prediction

Datasets: CNUHH (private dataset) and LUNG1 (publicly available dataset)

LUNG1:

-225 patient

-Data: clinical features (histology, age, gender, overall stage, T stage, M stage, N stage, smoking status, and smoking amount), death event, PET and RoI

CNUHH:

-442 patient

-Data: clinical features (histology, age, gender, overall stage, T stage, M stage, N stage), death event, CT and RoI

Table SI. Statistics of the CNUHH Dataset

Characteristic		Value	Characteristic		Value
Survival time (days)		628±481	Event (Death/Alive)		49/176
Age(years)		68.14±9.53	T stage	T1	55(24.44%)
Smoking amount		30.20±25.43		T2	112(49.78%)
Gender	Female	56(25.89%)		T3	36(16%)
	Male	169(75.11%)		T4	22(9.78%)
Histology	AD	122(54.22%)	N stage	N1	120(53.33%)
	SC	92(40.89%)		N2	33(14.67%)
	LC	5(2.22%)		N3	51(22.67%)
	NOS	6(2.67%)		N4	21(9.33%)
Overall stage	I	89(39.56%)	M stage	M1	255(100%)
	II	46(20.44%)		M2	0(0%)
	III	90(40%)	Smoking status	No	59(26.22%)
	IV	0(0%)		Yes	166(73.78%)

Table SII. Statistics of the LUNG1 Dataset

Characteristic		Value	Characteristic		Value
Survival time (days)		989±1036	Event (Death/Alive)		373/49
Age (years)		68.04±10.08	N stage	N1	170(40.28%)
Gender	Female	132(31.28%)		N2	23(5.45%)
	Male	290(68.72%)		N3	141(34.12%)
Histology	AD	51(12.09%)		N4	82(19.43%)
	SC	152(36.02%)	T stage	T1	93(22.04%)
	LC	114(27.01%)		T2	156(36.97%)
	NOS	63(14.93%)		T3	53(12.56%)
Overall stage	I	93(22.04%)		T4	117(27.73%)
	II	40(9.48%)		T5	2(0.47%)
	III	288(68.25%)	M stage	M1	417(98.82%)
	IV	0(0%)		M2	5(1.18%)

Non-small cell lung cancer prediction

Performance:

TABLE I
PERFORMANCE COMPARISON BETWEEN OUR PROPOSED METHOD AND THE COMPETING METHODS IN TUMOR SEGMENTATION TASK. (THE BEST RESULTS ARE MARKED BOLD)

Model	Dice score	
	CNUHH	LUNG1
UNet	0.6909 ± 0.0383	0.5059 ± 0.0354
ResUNet	0.7163 ± 0.0487	0.5310 ± 0.0390
MultiResUnet	0.6763 ± 0.0455	0.4892 ± 0.0364
TransUNet	0.6836 ± 0.0368	0.4792 ± 0.0253
MAPTransNet	$\mathbf{0.7261 \pm 0.0416}$	$\mathbf{0.5353 \pm 0.0349}$

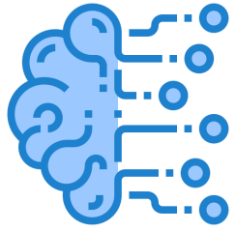
TABLE II
PERFORMANCE COMPARISON BETWEEN OUR PROPOSED METHOD AND THE CONVENTIONAL SURVIVAL ANALYSIS METHODS IN THE CNUHH DATASET . (THE BEST RESULTS ARE MARKED BOLD; *: GLOBAL CONTEXT FEATURES)

Method	C-Index	Brier	NBLL	MAE
Shape + Texture + Image [30]	0.7289	0.1477	0.4504	330
Clinical + Shape [38]	0.7796	0.1250	0.3925	312
Clinical + Shape + (PET-RoI)*	**0.8169**	**0.1180**	**0.3737**	**260**

TABLE III
PERFORMANCE COMPARISON BETWEEN OUR PROPOSED METHOD AND THE CONVENTIONAL SURVIVAL ANALYSIS METHODS IN THE LUNG1 DATASET . (THE BEST RESULTS ARE MARKED BOLD; *: GLOBAL CONTEXT FEATURES)

Type of Features	C-Index	Brier	NBLL	MAE
Shape + Texture + Image [30]	0.5569	0.1453	0.4555	539
Clinical + Shape [38]	0.5731	0.1447	0.4533	**532**
Clinical + Shape + (CT-RoI)*	**0.5860**	**0.1444**	**0.4489**	534

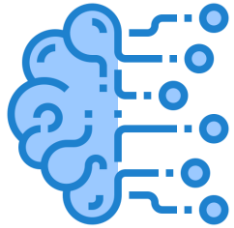

Thank You!



Publications

Articles in Peer-Reviewed Journals

- **Ho, N. H.**, Jeong, Y. H., & Kim, J. (2023). "Multimodal multitask learning for predicting MCI to AD conversion using stacked polynomial attention network and adaptive exponential decay". Scientific Reports, 13(1), 11243.
- Tran, T. D., **Ho, N. H.**, Pant, S., Yang, H. J., Kim, S. H., & Lee, G. (2023). "Cross-modality learning by exploring modality interactions for emotion reasoning". IEEE Access.
- **Ho, N. H.**, Yang, H. J., Kim, J., Dao, D. P., Park, H. R., & Pant, S. (2022). "Predicting progression of Alzheimer's disease using forward-to-backward bi-directional network with integrative imputation". Neural Networks, 150, 422-439.
- **Ho, N. H.**, Yang, H. J., Kim, S. H., Lee, G., & Yoo, S. B. (2021). "Deep Graph Fusion Based Multimodal Evoked Expressions From Large-Scale Videos". IEEE Access, 9, 127068-127080.
- Tran, T. D., Kim, J., **Ho, N. H.**, Yang, H. J., Pant, S., Kim, S. H., & Lee, G. S. (2021). "Stress analysis with dimensions of valence and arousal in the wild". Applied Sciences, 11(11), 5194.
- Tran, D. S., **Ho, N. H.**, Yang, H. J., Kim, S. H., & Lee, G. S. (2021). "Real-time virtual mouse system using RGB-D images and fingertip detection". Multimedia Tools and Applications, 80, 10473-10490.
- **Ho, N. H.**, Yang, H. J., Kim, S. H., & Lee, G. (2020). "Multimodal approach of speech emotion recognition using multi-level multi-head fusion attention-based recurrent neural network". IEEE Access, 8, 61672-61686.



Publications

Articles in Peer-Reviewed Journals

- Khanh, T. L. B., Dao, D. P., **Ho, N. H.**, Yang, H. J., Baek, E. T., Lee, G., ... & Yoo, S. B. (2020). "Enhancing U-Net with spatial-channel attention gate for abnormal tissue segmentation in medical imaging". Applied Sciences, 10(17), 5729.
- Tran, D. S., **Ho, N. H.**, Yang, H. J., Baek, E. T., Kim, S. H., & Lee, G. (2020). "Real-time hand gesture spotting and recognition using RGB-D camera and 3D convolutional neural network". Applied Sciences, 10(2), 722.
- **Ho, N. H.,** Yang, H. J., Kim, S. H., Jung, S. T., & Joo, S. D. (2019). "Regenerative semi-supervised bidirectional w-network-based knee bone tumor classification on radiographs guided by three-region bone segmentation". IEEE Access, 7, 154277-154289.
- Vu, T. D., **Ho, N. H.**, Yang, H. J., Kim, J., & Song, H. C. (2018). "Non-white matter tissue extraction and deep convolutional neural network for Alzheimer's disease detection". Soft Computing, 22, 6825-6833.
- Truong, P. H., Nguyen, N. D., **Ho, N. H.**, & Jeong, G. M. (2018). "Nonparametric regression-based step-length estimation for arm-swing walking using a smartphone". International Journal of Computers Communications & Control, 13(4), 566-573.
- **Ho, N. H.**, Truong, P. H., & Jeong, G. M. (2016). "Step-detection and adaptive step-length estimation for pedestrian dead-reckoning at various walking speeds using a smartphone". Sensors, 16(9), 1423.
- Ho, V. K., Doan, N. K., & **Ho, N. H.** (2015). Impact of Channel Estimation Error on the Performance of Relay Selection in Cognitive Radio Networks. Wireless Personal Communications, 84(4), 2513-2536.